DMD Fast Forward. Published on October 23, 2008 as DOI: 10.1124/dmd.108.022483
DMD Fast Forward. Published on October 23, 2008 as doi:10.1124/dmd.108.022483
This article has not been copyedited and formatted. The final version may differ from this version.

Disparity in intestine disposition between formed and preformed metabolites and implications: a theoretical study

Huadong Sun and K. Sandy Pang

Department of Pharmaceutical Sciences (H.S., K. S. P.),

Leslie Dan Faculty of Pharmacy, University of Toronto, Toronto, ON, M5S 3M2

Downloaded from dmd.aspetjournals.org at ASPET Journals on April 10, 2024

Copyright 2008 by the American Society for Pharmacology and Experimental Therapeutics.

DMD Fast Forward. Published on October 23, 2008 as DOI: 10.1124/dmd.108.022483
This article has not been copyedited and formatted. The final version may differ from this version.

Running Title Page

Running Title: Metabolite kinetics in intestine

Correspondence Author: Dr. K. Sandy Pang
Leslie Dan Faculty of Pharmacy
University of Toronto
144 College Street
Toronto, ON M5S 3M2 Canada
Tel: 416-978-6164
Fax: 416-978-8511
E-mail: ks.pang@utoronto.ca

Downloaded from dmd.aspetjournals.org at ASPET Journals on April 10, 2024

Abstract: 241 words

Number of text pages: 18

Introduction: 747 words

Discussion: 1349 words

References: 40

Figures: 10

Tables: 2

Abbreviations: TM, traditional model; SFM, segregated flow model; PBPK, physiologically-based pharmacokinetic model; AUC, area under the concentration-time curve; P, precursor; {pmi}, preformed metabolite; {mi,P} metabolite formed from precursor; {mi}, qualifier for metabolite (formed and preformed); CL_{d1} and CL_{d2}, basolateral, transfer intrinsic clearances between blood and tissue for theTM, or between blood and the enterocytes layer for the SFM; CL_{d3} and CL_{d4}, transfer intrinsic clearances between serosal blood and seroal tissue; $CL_{int,met,I}$, metabolic intrinsic clearance of precursor; $CL_{int,sec,I}$, secretory intrinsic clearance of precursor at the apical membrane; k_a, rate constant of absorption for precursor; k_g, rate constant of luminal transit and degradation; F_{abs}, fraction of drug absorbed from the intestinal lumen into intestine tissue; Q_I, Q_{en}, and Q_s, the blood flow for the whole intestine, enterocyte layer, and serosal layer, respectively.

DMD Fast Forward. Published on October 23, 2008 as DOI: 10.1124/dmd.108.022483
This article has not been copyedited and formatted. The final version may differ from this version.

Abstract

Metabolite in safety testing has been proposed for toxicity assessments. The question on how exposure of the synthetic metabolite compared to that of the formed metabolite was appraised kinetically using physiologically-based pharmacokinetic (PBPK) models, the (traditional) physiological model (TM) and segregated-flow (SFM) models. The SFM differs from the TM and describes a partial (~10% total) intestinal flow that perfuses the absorptive, metabolic, and secretory enterocyte layer so as to account for the higher extent of metabolism observed with oral vs. systemic dosing of drugs. Theoretical solutions for the areas under the curve of the formed metabolite after oral (po) and intravenous (iv) administration of the precursor (AUC{mi,P}) and preformed, synthetic metabolite (AUC{pmi}) showed identical AUC_{iv}{mi,P}, AUC_{po}{mi,P}, and AUC_{po}{pmi} for the TM and SFM, whereas a larger AUC_{iv}{pmi} existed for the SFM. The AUC{pmi} was influenced by metabolite parameters only: binding, absorptive (k_a{mi}) and luminal degradation (k_g{mi}) constants, intrinsic clearances for metabolism ($CL_{int,met,I}${mi}), apical efflux ($CL_{int,sec,I}${mi}), and basolateral transfer (CL_{d1}{mi} and CL_{d2}{mi}). By contrast, the AUC{mi,P} was influenced additionally by precursor parameters: rate constants k_a and k_g, and $CL_{int,met,I}$ and $CL_{int,sec,I}$, but not the basolateral transfer clearances. The drug parameters: $CL_{int,met,I}$ and k_a increased whereas $CL_{int,sec,I}$ decreased AUC{mi,P}, and secretion was counterbalanced by reabsorption with high k_as. The simulated time-courses and the AUC{pmi} and AUC{mi,P} resulting from iv and po routes of administration of preformed metabolite and precursor differed, inferring that the kinetics of the preformed and formed metabolites is not identical.

Downloaded from dmd.aspetjournals.org at ASPET Journals on April 10, 2024

DMD Fast Forward. Published on October 23, 2008 as DOI: 10.1124/dmd.108.022483
This article has not been copyedited and formatted. The final version may differ from this version.

INTRODUCTION

Metabolite-in-safety testing and the attainment of safe and efficacious drug use are key concerns in the drug development/surveillance paradigm. There has been a resurgence of interest on the testing of metabolites that are mediators of drug activity and toxicity due to the improvement in analytical methods for their detection, isolation, and characterization (Baillie et al., 2002). Metabolite testing is recommended, especially when metabolites are unique and identified only in humans, or when the metabolite exists at disproportionately higher levels in humans (>10%) than the animal species that was used for standard, nonclinical toxicology testing (Naito et al., 2007; FDA Guidance for Industry Safety Testing of Drug Metabolites, 2008). It has been proposed that a metabolite is considered as a major metabolite when the metabolite represents >10% (Davis-Bruno and Atrakchi, 2006), or 25% exposure of the precursor (Baillie et al., 2002). Others had suggested the estimate to be based on unbound concentration in the circulation or amounts in the excreta (Smith and Obach, 2005). When the "% exposure" is based on total radioactivity, the parameter is time-dependent, and may not be a reliable estimate when the metabolite in question is readily metabolized to other metabolites. Many commentaries suggest that the definition of the % exposure or amount may not be the key issue. Rather, testing needs to be appraised case-by-case (Hastings et al., 2003; Humphreys and Unger, 2006; Naito et al., 2007; FDA Guidance for Industry Safety Testing of Drug Metabolites, 2008).

Obviously, it is virtually impossible to synthesize reactive or unstable metabolites for the proper characterization of toxicity. Suffice to say, the metabolite must be stable. An important question for stable, synthetically-prepared metabolite is how to administer the in order to mimic exposure of the formed metabolite. Would the time-course and AUC of the

Downloaded from dmd.aspetjournals.org at ASPET Journals on April 10, 2024

DMD Fast Forward. Published on October 23, 2008 as DOI: 10.1124/dmd.108.022483
This article has not been copyedited and formatted. The final version may differ from this version.

preformed metabolite be similar to the time-course and AUC of the formed metabolite and mimic metabolite exposure from precursor drug administration?

The ADME properties of the precursor drug and metabolite would need to be considered for metabolite kinetics. Our laboratory had employed perfused organ approaches to examine metabolite kinetics in the liver (deLannoy et al., 1993) and kidney (Geng et al., 1996) after administrations of both the drug and preformed metabolite. Differences were found between the fates of the generated and preformed metabolites upon solving for the AUC of the formed vs. the preformed metabolite (Pang et al., 2008). Transporters and enzymes of the parent drug and metabolite were found to be important variables that determine the AUC of the formed metabolite, AUC{mi,P}. But the drug parameters were absent regarding the AUC of the preformed metabolite, AUC{pmi}, in both the liver and kidney.

The theoretical examination of metabolite disposition has not been extended to the intestine, although there has been development on modeling of transporters and/or enzymes for drug absorption (Cong et al., 2000, Kothare and Zimmerman 2002). In this tissue, apical absorptive transporters bring molecules into the enterocyte whereas apical efflux transporters are capable of secreting the absorbed drug back to the lumen, and the drug in tissue is subject to biotransformation before it enters the circulation at the basolateral membrane, either passively or via efflux transporters (Pang, 2003). The net outcome of the events constitutes intestinal drug absorption.

In this communication, we tested the hypotheses that precursor and metabolite parameters influence the kinetics of the formed metabolite, and that differences exist between preformed and formed metabolite kinetics in the intestine. Two physiologically-based pharmacokinetic (PBPK) models are used. The traditional physiological model (TM) (Figure 1A) has identified parameters

Downloaded from dmd.aspetjournals.org at ASPET Journals on April 10, 2024

DMD Fast Forward. Published on October 23, 2008 as DOI: 10.1124/dmd.108.022483
This article has not been copyedited and formatted. The final version may differ from this version.

of gastrointestinal transit, intestinal flow, and intestinal transporters and enzymes as variables that regulate the ultimate absorption of orally administered substrates. The segregated flow model (SFM) suggests that a minor proportion of the intestinal flow perfuses the enterocyte region that mediates absorption, metabolism, and efflux, and a larger flow perfuses a non-metabolizing (inert) serosal tissue (Figure 1B). Both models are presently extended to describe metabolite kinetics so as to identify parameters that would affect the AUC of the formed and preformed metabolites for oral and intravenous administration. The SFM is necessary to explain the greater extent of intestinal metabolism that is associated with oral dosing compared to systemic dosing. This route-dependent, intestinal metabolism was observed for morphine (Cong et al., 2000) and other substrates in both animals and man (Pang, 2003). Not unlike the SFM, SimCYP®, the simulation program, uses a strategy based on a reduced villous flow and not total intestinal flow for the prediction of intestinal clearances (Yang et al., 2007).

Downloaded from dmd.aspetjournals.org at ASPET Journals on April 10, 2024

DMD Fast Forward. Published on October 23, 2008 as DOI: 10.1124/dmd.108.022483
This article has not been copyedited and formatted. The final version may differ from this version.

METHODS

The TM and SFM models are physiologically-based models that have been introduced to relate flow, volume, transporters that mediate absorption, distribution and secretion, and enzymes for metabolism (Fig. 1) (Cong et al., 2000). The need for comparing metabolite kinetics for the TM and SFM is based on the superiority of the SFM in explaining route-dependent intestinal metabolism, that less drug is metabolized with intravenous vs. oral drug administration (Cong et al., 2000). This concept was also adopted by SimCYP® in the modeling of intestinal clearances with a villous flow (Q_{villi}) which is lower compared to the total intestinal flow (Yang et al., 2007).

For the TM, the total intestinal blood (Q_I) perfuses the entire intestinal tissue; the transfer intrinsic clearances for the transport of precursor (P) between blood and tissue at the basolateral membrane are described by CL_{d2} and CL_{d1}, representing the summation of passive and transporter-mediated pathways. In tissue, metabolism (intrinsic clearance, $CL_{int,met,I}$) to form the primary metabolite, Mi, and apical secretion into the lumen (secretory intrinsic clearance, $CL_{int,sec,I}$) are available elimination processes (Fig. 1A). In the lumen, the precursor drug may be absorbed (rate constant, k_a) or leave the lumen irreversibly via gastrointestinal transit or degradation (rate constant, k_g). The fraction of dose absorbed, F_{abs}, is given by $k_a/(k_a+k_g)$ and describes the net extent of intestinal absorption into the intestinal tissue.

For the SFM, the intestinal blood flow is segregated, with a lower flow (Q_{en}, 10% total intestinal flow) perfusing the enterocyte region that consists of apical and basolateral transporters and metabolic enzymes. The remaining, seroal flow (Q_s, 90% flow) perfuses a non-metabolizing or inert region (serosa, submucosa and part of the mucosa) (Cong et al., 2000) (Fig. 1B). Subscripts enb, en, sb, and s, denoting enterocyte blood, enterocyte tissue, serosal blood, and

Downloaded from dmd.aspetjournals.org at ASPET Journals on April 10, 2024

DMD Fast Forward. Published on October 23, 2008 as DOI: 10.1124/dmd.108.022483
This article has not been copyedited and formatted. The final version may differ from this version.

serosal tissue, respectively, are used to describe parameters for flow and volume for the precursor, P, and the primary metabolite, Mi. The drug exchanges between blood and the corresponding tissue layers with transfer clearances, CL_{d1} and CL_{d2} for the enterocyte region and CL_{d3} and CL_{d4} for the serosal region (Fig. 1). A similar set of parameters exists for the metabolite. The parameters of the precursor are not qualified, whereas those for the metabolite are qualified by {mi}; those pertaining specifically for the preformed and formed metabolites are further classified by {pmi} and {mi,P}, respectively.

These models were utilized to build concepts on metabolite kinetics. For simplicity, the intestine was assumed to be the only tissue for metabolism, secretion, as well as absorption, and PBPK modeling was based on the perfused rat intestine preparation. Binding of the drug and metabolite was assumed as non-existent (unbound fractions = unity), and it was assumed that the P formed only one primary metabolite (Mi), which underwent further metabolism and secretion in the intestine (Fig. 1). It was assumed that activities for absorption (k_a{mi}), luminal degradation and gastrointestinal transit (k_g{mi}), transport (CL_{d1}{mi}, CL_{d2}{mi}, C_{Ld3}{mi}, and CL_{d4}{mi}), secretion ($CL_{int,sec,I}${mi}) and metabolism ($CL_{int,met,I}${mi}) are identical for both preformed and formed metabolites.

Rate-equations pertaining to the rates of change of precursor and metabolite were presented in the Appendix under linear conditions. The coefficients were used for matrix inversion by the program, Maple9® (Waterloo Maple Inc., Waterloo, Canada). The solutions provided the areas under the concentration time curve of the preformed (AUC{pmi}) and formed (AUC{mi,P}) primary metabolites after administration of the synthetic metabolite and precursor drug (doses of 100 units into a reservoir volume of 200 ml and luminal volume of 2 ml), respectively. Accordingly, the unit of metabolite concentration in the reservoir is dose unit/ml

Downloaded from dmd.aspetjournals.org at ASPET Journals on April 10, 2024

DMD Fast Forward. Published on October 23, 2008 as DOI: 10.1124/dmd.108.022483
This article has not been copyedited and formatted. The final version may differ from this version.

and the unit of AUC is dose unit/ml·min. The solutions were in turn used to examine the influence of flow (total intestinal flow, Q_I = 8 ml/min for the TM, and Q_{en} = 0.8 ml/min and Q_s = 7.2 ml/min for the SFM), transfer (CL_{d1}{mi} and CL_{d2}{mi}, from 0.01 to 2 ml/min), intestinal metabolism ($CL_{int,met,I}$ and $CL_{int,met,I}${mi}, from 0 to 1 ml/min), secretion ($CL_{int,sec,I}$ and $CL_{int,sec,I}${mi}, from 0 to 1 ml/min), absorption (k_a and k_a{mi}, from 0.01 to 1 min^{-1}), and luminal degradation/transit (k_g and k_g{mi} from 0 to 0.2 min^{-1}) parameters of the precursor (not qualified) and metabolite (qualified by {mi}) on AUC{mi,P} and AUC{pmi}. The simulated AUCs highlighted differences between the preformed {pmi} and formed {mi,P} metabolites with respect to different routes of administration of the precursor drug and preformed metabolite, and identified the sensitivity of the AUC of the metabolite, formed and preformed, to the various parameters.

Numerous conditions may also be used to simulate concentration-time profiles of the formed and preformed metabolites. However, it was not feasible to display all of the conditions. Simulations were confined only to several examples to illustrate the important features (Table 1). The time-course of preformed and formed metabolites were compared for the TM and SFM for both intravenous and oral dosing by varying the k_a of the precursor, and the transfer clearances CL_{d1}{mi},CL_{d2}{mi}, CL_{d3}{mi}, and CL_{d4}{mi}, or CL_d{mi}). Simulations were conducted with the program, Scientist® (St Louis, MO) with differential equations shown in the Appendix. Cases 1 and 2 represented extreme cases for metabolite transport, at CL_{d1}{mi}, CL_{d2}{mi}, CL_{d3}{mi}, and CL_{d4}{mi} = 2 and 0.01 ml/min, respectively, denoting a high vs. low value transfer clearances for the metabolite; the precursor transfer clearances were assumed to be identical and were assigned the higher value (CL_d = 2 ml/min). The absorption rate constant of the precursor,

Downloaded from dmd.aspetjournals.org at ASPET Journals on April 10, 2024

DMD Fast Forward. Published on October 23, 2008 as DOI: 10.1124/dmd.108.022483
This article has not been copyedited and formatted. The final version may differ from this version.

k_a, was changed from 0.01 to 0.05 and 1 min^{-1}, and $k_a\{mi\}$ was changed from 0.05 to 0.01 and 0.000001 min^{-1}.

Downloaded from dmd.aspetjournals.org at ASPET Journals on April 10, 2024

DMD Fast Forward. Published on October 23, 2008 as DOI: 10.1124/dmd.108.022483
This article has not been copyedited and formatted. The final version may differ from this version.

RESULTS

The following solutions for AUC{mi,P} and AUC{pmi} for intravenous (subscripted iv) or oral (subscripted po) administration of the precursor and preformed metabolite, respectively, for the TM and SFM were obtained from matrix inversion by Maple®.

$$AUC_{iv}^{TM}\{pmi\} = \frac{Dose_{iv}\{pmi\}\left[\left(1-F_{abs}\{mi\}\right)CL_{int,sec,I}\{mi\}\left(Q_I+CL_{d1}\{mi\}\right)+Q_I\left(CL_{d2}\{mi\}+CL_{int,met,I}\{mi\}\right)+CL_{d1}\{mi\}CL_{int,met,I}\{mi\}\right]}{Q_I CL_{d1}\{mi\}\left[\left(1-F_{abs}\{mi\}\right)CL_{int,sec,I}\{mi\}+CL_{int,met,I}\{mi\}\right]} \quad (1)$$

$$AUC_{iv}^{SFM}\{pmi\} = \frac{Dose_{iv}\{pmi\}\left[\left(1-F_{abs}\{mi\}\right)CL_{int,sec,I}\{mi\}\left(Q_{en}+CL_{d1}\{mi\}\right)+Q_{en}\left(CL_{d2}\{mi\}+CL_{int,met,I}\{mi\}\right)+CL_{d1}\{mi\}CL_{int,met,I}\{mi\}\right]}{Q_{en}CL_{d1}\{mi\}\left[CL_{int,sec,I}\{mi\}\left(1-F_{abs}\{mi\}\right)+CL_{int,met,I}\{mi\}\right]} \quad (2)$$

$$AUC_{po}^{TM\text{ and }SFM}\{pmi\} = \frac{Dose_{po}\{pmi\}F_{abs}\{mi\}CL_{d2}\{mi\}}{CL_{d1}\{mi\}\left[\left(1-F_{abs}\{mi\}\right)CL_{int,sec,I}\{mi\}+CL_{int,met,I}\{mi\}\right]} \quad (3)$$

$$AUC_{iv}^{TM\text{ and }SFM}\{mi,P\} = \frac{Dose_{iv}CL_{int,met,I}CL_{d2}\{mi\}}{CL_{d1}\{mi\}\left[\left(1-F_{abs}\{mi\}\right)CL_{int,sec,I}\{mi\}+CL_{int,met,I}\{mi\}\right]\left[(1-F_{abs})CL_{int,sec}+CL_{int,met,I}\right]} \quad (4)$$

$$AUC_{po}^{TM\text{ and }SFM}\{mi,P\} = \frac{Dose_{po}CL_{d2}\{mi\}F_{abs}CL_{int,met,I}}{CL_{d1}\{mi\}\left[\left(1-F_{abs}\{mi\}\right)CL_{int,sec,I}\{mi\}+CL_{int,met,I}\{mi\}\right]\left[(1-F_{abs})CL_{int,sec}+CL_{int,met,I}\right]} \quad (5)$$

The above equations for the formed metabolite were found to differ from those for the preformed metabolite when doses of the performed metabolite (Dose{pmi}) or precursor (Dose) were given intravenously (iv) or orally (po) (Table 2). It was also noted in all of the above solutions that the $CL_{int,sec,I}$ and $CL_{int,sec,I}\{mi\}$ terms were effectively reduced by $(1\text{-}F_{abs})$ and $(1\text{-}F_{abs}\{mi\})$,

Downloaded from dmd.aspetjournals.org at ASPET Journals on April 10, 2024

DMD Fast Forward. Published on October 23, 2008 as DOI: 10.1124/dmd.108.022483
This article has not been copyedited and formatted. The final version may differ from this version.

respectively, suggesting that intestinal reabsorption effectively reduced the luminal, secretory activity. The equations on the AUCs for drug and formed metabolite may be used to predict changes in transporter and/or enzyme and the associated intrinsic clearances or activities, and should be useful to predict transporter-transporter and enzyme-transporter interplay and drug-drug interactions.

AUC_{iv}{pmi}, AUC_{po}{pmi} and F{pmi} after administration of preformed metabolite. The drug parameters: $CL_{int,met,I}$, $CL_{int,sec,I}$, CL_{d1}, CL_{d2}, k_a, and k_g, were absent in the solutions for the preformed metabolite, AUC_{iv}{pmi} and AUC_{po}{pmi} (Eqs. 1 to 3). The AUC_{po}{pmi} for the TM and SFM was identical, whereas differences existed for AUC_{iv}{pmi} due to difference in the flow terms: Q_I for TM and Q_{en} for the SFM (Eqs. 1 and 2), as described previously by Cong et al. (2000). Since the flow terms were absent in the solution for AUC_{po}{pmi}, the same solution (Eq. 3) existed for the TM and SFM.

Simulations that were based on Eq. 1 and 2 revealed similar profiles for AUC_{iv}{pmi} for the TM and SFM, when $CL_{int,met,I}${mi} and $CL_{int,sec,I}${mi} were altered. The resulting AUC_{iv}{pmi} was lower for the TM due to the higher flow rate ($Q_I > Q_{en}$) (Fig. 2). Increasing $CL_{int,met,I}${mi} or $CL_{int,sec,I}${mi} decreased the AUC_{iv}{pmi}, and the effect was greater for the TM than the SFM. Comparatively speaking, $CL_{int,met,I}${mi} reduced AUC_{iv}{pmi} more so than $CL_{int,sec,I}${mi} for both the TM (Figs. 2A and 2C) and the SFM (Figs. 2B and 2D). Values of AUC_{iv}{pmi} were dramatically higher with lower transfer clearances of the metabolite that tended to bar the metabolite from entry into enterocytes (cf. CL_d{mi}s at 2 vs. 0.01 ml/min). The rate constant k_a{mi} and the F_{abs}{mi} affected the AUC{pmi} for both oral and intravenous metabolite dosing. The metabolite that was secreted into the lumen was subject to reabsorption, rendering higher AUC_{iv}{pmi}s with high k_a{mi}s, regardless of whether the preformed metabolite was given

Downloaded from dmd.aspetjournals.org at ASPET Journals on April 10, 2024

DMD Fast Forward. Published on October 23, 2008 as DOI: 10.1124/dmd.108.022483
This article has not been copyedited and formatted. The final version may differ from this version.

orally or intravenously (Fig. 3). This effect explained why there were greater changes associated with $CL_{int,met,I}\{mi\}$ than with $CL_{int,sec,I}\{mi\}$ for both iv (Fig. 2) and po (Fig. 4A) administration of the metabolite. Secretion was effectively reduced by avid reabsorption (high $k_a\{mi\}$) to negate the effects of metabolite secretion ($CL_{int,sec,I}\{mi\}$) (Fig. 4B); these patterns were generally similar to that of $AUC_{iv}\{pmi\}$ (Figs. 2 and 3). The luminal removal constant of the metabolite, $k_g\{mi\}$, tended to remove the secreted metabolite, thereby decreasing both $AUC_{iv}\{pmi\}$ and $AUC_{po}\{pmi\}$ (simulations not shown). Values of $AUC_{po}\{pmi\}$ changed proportionally with the ratio, $CL_{d2}\{mi\}/CL_{d1}\{mi\}$, regardless of the absolute values of $CL_{d2}\{mi\}$ and $CL_{d1}\{mi\}$: the greater the ratio, the greater the $AUC_{po}\{pmi\}$ (Fig. 4C).

Values of F{pmi}, obtained as the ratio, $AUC_{po}\{pmi\}/AUC_{iv}\{pmi\}$, also displayed similar patterns as those of AUC{pmi} with respect to the greater sensitivity to $CL_{int,met,I}\{mi\}$, but less so with $CL_{int,sec,I}\{mi\}$. Values of F{pmi} were generally higher for the TM over the SFM for the same set of variables (compare Figs. 5A and 5B), and reabsorption of the metabolite tended to neutralize the effect of secretion of the metabolite. At low transport clearances, absorption was greatly affected, rendering much lower F{pmi} (Figs 5C and 5D). Higher values of F{pmi} were apparent with higher $CL_{d2}\{mi\}$ and reduced $CL_{d1}\{mi\}$ (simulations not shown).

$AUC_{iv}\{mi,P\}$ and $AUC_{po}\{mi,P\}$ after administration of precursor drug. Solutions for $AUC_{iv}\{mi,P\}$ the formed metabolite for the TM were identical to that of the SFM (Eq. 4). The same comment also applied to $AUC_{po}\{mi,P\}$ (Eq. 5). These areas of the formed metabolite ($AUC_{iv}\{mi,P\}$ and $AUC_{po}\{mi,P\}$) arising from precursor administration were further affected by precursor drug parameters for metabolism and secretion ($CL_{int,met,I}$ and $CL_{int,sec,I}$), and the fraction of precursor dose absorbed (F_{abs}). In addition, $AUC_{iv}\{mi,P\}$ and $AUC_{po}\{mi,P\}$ were also modulated by metabolite parameters: $k_a\{mi\}$ and $k_g\{mi\}$ that affect $F_{abs}\{mi\}$, the metabolite

Downloaded from dmd.aspetjournals.org at ASPET Journals on April 10, 2024

DMD Fast Forward. Published on October 23, 2008 as DOI: 10.1124/dmd.108.022483
This article has not been copyedited and formatted. The final version may differ from this version.

transfer clearances, $CL_{d1}\{mi\}$ and $CL_{d2}\{mi\}$, and the metabolite intrinsic clearances, $CL_{int,met,I}\{mi\}$ and $CL_{int,sec,I}\{mi\}$ (Eqs. 4 and 5).

Expectedly, increasing $CL_{int,met,I}$ values led to increased $AUC_{iv}\{m,P\}$ (Fig. 6A) and $AUC_{po}\{mi,P\}$ (Fig. 6B), whereas increasing the intrinsic activity of the competing secretion pathway of the precursor ($CL_{int,sec,I}$) decreased both the $AUC_{iv}\{m,P\}$ and $AUC_{po}\{mi,P\}$. Again, the effects of precursor secretion could be alleviated by high k_a values (Fig. 6C and 6D). Changes in $CL_{int,met,I}\{mi\}$ affected the $AUC_{iv}\{mi,P\}$ and $AUC_{po}\{mi,P\}$ more than from $CL_{int,sec,I}\{mi\}$ (Figs. 7A and 7B). Changes in metabolite transport also affected the AUCs{mi,P}; an increase in $CL_{d2}\{mi\}$ or decrease in $CL_{d1}\{mi\}$, as well as increase in $k_a\{mi\}$ increased both $AUC_{iv}\{mi,P\}$ and $AUC_{po}\{mi,P\}$ (simulation on ratio of transfer clearances, shown in Figs. 7C and 7D). It was noted that the ratio, $AUC_{po}\{mi,P\}/AUC_{iv}\{mi,P\}$, was the fraction of precursor absorbed, F_{abs} (Table 2).

Comparison of AUCs of the metabolites. The solutions of the AUCs of the formed and preformed metabolites allowed a comparison of the areas for the TM and SFM with respect to different routes of administration (Table 2). The ratios of areas for the formed to preformed metabolite after iv and po administration of precursor and preformed metabolite, $[AUC_{iv}\{mi,P\}/AUC_{iv}\{pmi\}]$ and $[AUC_{po}\{mi,P\}/AUC_{po}\{pmi\}]$, were not unity (Table 2). $F\{pmi\}$, given by the ratio, $[AUC_{iv}\{mi,P\}/AUC_{iv}\{pmi\}]$, exhibited different sensitivities to the metabolite parameters for the TM and SFM; this was again due to the flow terms Q_I and Q_{en}. The area ratio of $AUC_{po}\{mi,P\}/AUC_{iv}\{mi,P\}$ for both TM and SFM yielded a simplified $F_{abs}Dose_{po}/Dose_{iv}$ and was reduced to F_{abs} or $[k_a/(k_a+k_g)]$ when equal precursor doses were administered (Table 2).

Downloaded from dmd.aspetjournals.org at ASPET Journals on April 10, 2024

DMD Fast Forward. Published on October 23, 2008 as DOI: 10.1124/dmd.108.022483
This article has not been copyedited and formatted. The final version may differ from this version.

Simulations on time course of preformed and formed metabolites. Cases 1 and 2 (Table 1) represented divergent cases on metabolite transport [$CL_d\{mi\} = CL_{d1}\{mi\} = CL_{d2}\{mi\} = CL_{d3}\{mi\} = CL_{d4}\{mi\}$= 2 and 0.01 ml/min] and precursor absorption [(k_a = 0.01 and 1 min^{-1}) on the concentration-time profiles of the preformed (Fig. 8) and formed (Fig. 9) metabolites. Simulations for the preformed metabolite after its iv administration revealed a faster decay profile for preformed metabolite for the TM when compared to the SFM (Figs. 8A). This is expected due to the greater intestinal clearance based on Q_I and not Q_{en}, yielding a lower $AUC_{iv}\{pmi\}$ for the TM. With po dosing, the peak concentration of the preformed metabolite was lower according to the SFM and this occurred at almost the same time as that for the TM; the decay $t_{1/2}$ of the metabolite for the SFM was also longer. The TM metabolite profile crossed over that of the SFM, and the $AUC_{po}\{pmi\}$s for both the TM and SFM were identical. The pattern existed for all $CL_d\{mi\}$ values of the metabolite. Poor transfer characteristics of the metabolite into the enterocyte transformed the decay profile to yield a protracted $t_{1/2}$, showing the strong influence of the metabolite transfer clearances (cf. Figures 8A and 8B). Under the condition of poor metabolite entry, there was virtually no difference in the decay profiles of the preformed metabolite between the TM and SFM. Note also that the $t_{1/2}$s for the iv and po cases for the TM or SFM were parallel (Fig. 8).

Profiles of the formed metabolite were found to alter with the absorption rate constant of the precursor, k_a, and the metabolite transfer clearance, $CL_d\{mi\}$(Fig. 9). At high $CL_d\{mi\}$ and low absorption rate constant (k_a = 0.01 min^{-1}), levels of the formed metabolite for the TM and the SFM after iv precursor administration were generally higher than those after po dosing. At high $CL_d\{mi\}$ and high k_a (1 min^{-1}), the concentration-time profiles of the metabolite edged closer for both iv and po precursor doses, although the metabolite profiles after po peaked earlier than those

Downloaded from dmd.aspetjournals.org at ASPET Journals on April 10, 2024

DMD Fast Forward. Published on October 23, 2008 as DOI: 10.1124/dmd.108.022483
This article has not been copyedited and formatted. The final version may differ from this version.

for iv (Fig 9B). At low $CL_d\{mi\}$s, however, only upswing profiles were observed for the simulated cases at both the low (0.01 min^{-1}) and high (1 min^{-1}) k_as (Figs. 9C and 9D). The metabolite profiles after iv precursor administration were comparatively higher than those for oral dosing of precursor that exhibited poor absorption (k_a= 0.01 min^{-1}) (Fig. 9C). With good precursor absorption (k_a = 1 min^{-1}), all metabolite profiles became comparable (Fig. 9D) when reabsorption reclaimed most of the secreted precursor. Generally speaking, the formed metabolite peaked earlier and higher with increasing k_a, since a faster precursor absorption rate not only increased the rate of drug delivery to intestinal enzyme sites but also reduced effectively the secretory intrinsic clearance, $CL_{int,sec,I}$ (see Table 2). Because $AUC_{iv}\{mi,P\}$ is identical for the TM and SFM, the metabolite curves eventually crossed over, and the $AUC_{iv}\{mi,P\}$s became identical (Fig. 9); the same occurred for $AUC_{po}\{mi,P\}$.

Simulations based on equivalent preformed metabolite dose. One strategy was formulated to estimate the dose equivalent of the preformed metabolite that would yield an AUC{pmi) identical to the AUC{mi,P} (precursor Dose = 100 units). From Table 2, the required doses, $Dose_{iv}\{pmi\}$ and $Dose_{po}\{pmi\}$, can be calculated.

For the TM, iv case

$$Dose_{iv}\{pmi\}=\frac{Dose_{iv}Q_I CL_{int,met,I} CL_{d2}\{mi\}}{\left((1-F_{abs})CL_{int,sec,I}+CL_{int,met,I}\right)\left((1-F_{abs}\{mi\})CL_{int,sec,I}\{mi\}\left[CL_{d1}\{mi\}+Q_I\right]+Q_I\left[CL_{d2}\{mi\}+CL_{int,met,I}\{mi\}\right]+CL_{d1}\{mi\}CL_{int,met,I}\{mi\}\right)} \quad (6)$$

and for the SFM, iv case

$$Dose_{iv}\{pmi\}=\frac{Dose_{iv}Q_{en} CL_{int,met,I} CL_{d2}\{mi\}}{\left((1-F_{abs})CL_{int,sec,I}+CL_{int,met,I}\right)\left((1-F_{abs}\{mi\})CL_{int,sec,I}\{mi\}\left[CL_{d1}\{mi\}+Q_{en}\right]+Q_{en}\left[CL_{d2}\{mi\}+CL_{int,met,I}\{mi\}\right]+CL_{d1}\{mi\}CL_{int,met,I}\{mi\}\right)} \quad (7)$$

Downloaded from dmd.aspetjournals.org at ASPET Journals on April 10, 2024

DMD Fast Forward. Published on October 23, 2008 as DOI: 10.1124/dmd.108.022483
This article has not been copyedited and formatted. The final version may differ from this version.

For both the TM and SFM, po cases

$$Dose_{po}\{pmi\} = \frac{Dose_{po} F_{abs} CL_{int,met,I}}{F_{abs}\{mi\}\left[(1-F_{abs})CL_{int,sec,I} + CL_{int,met,I}\right]} \quad (8)$$

Simulations of the most likely case of preformed metabolite administration, the oral case, required an estimate of $Dose_{po}\{pmi\}$, as shown in Eq. 8 [$AUC_{po}\{pmi) = AUC_{po}\{mi,P)$]. Simulations derived thereafter showed consistently lower profiles of the formed metabolite vs. those for the preformed metabolite, especially at the earlier times for all of the cases simulated (Fig. 10). These patterns held regardless of k_a (0.01 or 1 min^{-1}) (cf. Figs. 10A and 10B and Figs. 10C and 10D), or $CL_d\{mi\}$ (2 or 0.01 ml/min) (Figs 10A and 10B vs. Figs. 10C and 10D). The influence of $k_a\{mi\}$ was also examined. Upon decreasing $k_a\{mi\}$, the required $Dose_{po}\{pmi\}$, according to Eq. 8, needed to be increased accordingly. The resulting simulations at low $k_a\{mi\}$ showed profiles that were similar to those in Fig. 10, although the metabolite concentrations were lower (simulations not shown).

Downloaded from dmd.aspetjournals.org at ASPET Journals on April 10, 2024

DMD Fast Forward. Published on October 23, 2008 as DOI: 10.1124/dmd.108.022483
This article has not been copyedited and formatted. The final version may differ from this version.

DISCUSSION

The aspect on drug safety impacts on preclinical and clinical stages in drug development and extends to the time when the drug is in the market place. In vitro testing and in vivo pharmacokinetics either in animals or in man is of paramount importance. These include in silico testing, high throughput systems that are enzyme- or cell-based, including microfluidic systems of multiple cells in culture (Leeder et al., 1989; Johansson et al., 2004; Kehtani and Bhatia, 2006; Li, 2007), and identification of mechanisms of on-target and off-target toxicity via covalent binding, alkylation protein, DNA (Baillie, 2006) or downstream adducts, biomarkers, or mechanism-based inactivation of cytochrome P450s (Jones et al., 2007). Animal models and surrogate animal testing are utilized for investigation of metabolite-mediated toxicity, genotoxicity studies, toxicity testing of embryonic-fetal development, and carcinogenicity studies in toxicological testing (Stevens, 2006; Lee and Dordick 2006). In cases where metabolite exposure has been inadequately assessed, it is proposed that synthesized reference standard may need to be prepared and the safety of the metabolite assessed using a route of administration whereby adequate exposure can be obtained in an appropriate species (FDA Guidance, 2008).

The recent 2008 FDA guidance on metabolite safety defined a major metabolite as 10%. It is unknown whether this value is based on the percent of total radioactivity in serum, excreta, dose, or the AUC of the parent drug. The estimate of the metabolite amount is imprecise even with use of a radioactivity dose, since the value is time-dependent and reliant on the eliminatory pathways of the metabolite. The latter method necessitates consideration of a sound estimate for the volume of distribution of the metabolite. This distribution volume of the formed metabolite may or may not be identical to that obtained from administration of the preformed metabolite. Moreover, metabolite testing has been proposed, even though it has

Downloaded from dmd.aspetjournals.org at ASPET Journals on April 10, 2024

DMD Fast Forward. Published on October 23, 2008 as DOI: 10.1124/dmd.108.022483
This article has not been copyedited and formatted. The final version may differ from this version.

been recognized that direct dosing of the metabolite may lead to subsequent metabolism that may lead to formation of other metabolites which does not reflect the situation clinically, thereby complicating the toxicity picture (Smith and Obach, 2006; Prueksaritoanont et al., 2006; Pang et al., 2008). A reverberating theme that came through is that the safety assessment of metabolite should be a case-by-case approach (Kastings et al., 2003; Naito et al., 2007, FDA Guidance, 2008).

If metabolite testing is mandated in animal testing or man, an inevitable question is how to administer the metabolite, systemically or orally. From a theoretical standpoint, there is the need to consider the SFM in addition to the TM for intestinal modeling, since many drugs are shown to exhibit intestinal route-dependent metabolism (Pang, 2003). A similar strategy was utilized by the SimCYP® group to describe intestinal clearances (Yang et al., 2007). Therefore, we felt compelled to compare the results on AUC{mi,P} for both the TM and the SFM, expecting to see higher AUC_{iv}{pmi} for the SFM due to the flow differences, Q_{en} for the SFM and Q_I for the TM (Table 2). We showed that formed and preformed metabolite kinetics and time-courses differed in the intestine, and these were dependent on the route of administration and flow patterns (Q_I vs. Q_{en}) of the intestine (Figs. 2 to 10). The AUC_{po}{pmi} were identical for both models. Moreover, identical AUC{mi,P}s were found for the TM and SFM for iv precursor administration, and the same applied to po administration as well. The time courses of the formed metabolite were found to differ with different k_a of the precursor (Fig, 9). Even when "area-equivalent" preformed metabolite oral doses were given, the correspondence between the formed and preformed metabolite levels was poor, especially for the early time points (Fig. 10).

The results showed that, in consideration of intestinal elimination only, the resulting AUC{pmi} was affected only by the absorptive, distributional and eliminatory characteristics of

Downloaded from dmd.aspetjournals.org at ASPET Journals on April 10, 2024

DMD Fast Forward. Published on October 23, 2008 as DOI: 10.1124/dmd.108.022483
This article has not been copyedited and formatted. The final version may differ from this version.

the metabolite, whereas AUC{mi,P} was additionally influenced by the absorptive and eliminatory characteristics of the precursor. Upon comparison, the AUC{mi,P} differed from AUC{pmi} for the oral and intravenous cases for both models (Table 2). The same was found in the liver and kidney. The areas under the curve of the formed metabolite were influenced by distributional and eliminatory characteristics of both the precursor and metabolite in the organ, suggesting that metabolite administration will lead to kinetic observations that deviate from those of the preformed metabolite (Pang et al., 2008). Indeed, evidence on different kinetics between the formed species was found to exist in the liver (Xu et al., 1990; deLannoy et al., 1993), kidney (Geng et al., 1996), and intestine (Cong et al., 2000).

The time-course of the toxic, formed metabolite and its AUC{mi,P} would be influenced by distributional and eliminatory characteristics of the metabolite in the intestinal tissue, and those for the precursor (Figs. 8 to10), the route of administration and whether a partial or total flow perfuses the enterocyte region (TM vs. SFM). The notion that exposure of the metabolite is reproducible by administration of the preformed metabolite is not attainable, and there was practical limitations in this approach. The same was implied in a commentary by Smith and Obach (2006). However, the argument of %exposure vs. absolute amount (Baillie et al., 2002; Smith and Obach, 2005; 2006) is immaterial and irrelevant in providing any clearer answers. More relevant is how to mimic the kinetics and toxicity of the metabolite in question.

The theoretical examination has alluded to the dilemma in metabolite toxicity testing with testing of synthetic metabolites. There are additional features that can modulate metabolite AUCs presented in this theoretical treatise. First, the heterogeneous distribution of transporters and enzymes along the segment of the small intestine has been shown to influence drug bioavailability (Pang, 2003; Tam et al., 2003, Liu et al., 2006). There heterogeneous distribution

Downloaded from dmd.aspetjournals.org at ASPET Journals on April 10, 2024

DMD Fast Forward. Published on October 23, 2008 as DOI: 10.1124/dmd.108.022483
This article has not been copyedited and formatted. The final version may differ from this version.

of enzymes in the liver has been known to result in dramatically different fates of administered and formed primary metabolites (Xu et al., 1990; Tan and Pang, 2001; Pang et al., 2008). The metabolite profiles will change when metabolite formation occurs in multiple organs (deLannoy and Pang, 1993), or when there is sequential handling of the formed, primary metabolite in other downstream or parallel organs (e.g. intestinally formed, primary metabolites undergo hepatic metabolism prior to reaching the systemic circulation). Transport characteristics of the primary metabolite in each organ involved in formation or further metabolism could differ and result in differences in metabolite AUC.

Although metabolite administration/testing would not directly reflect the time course of the formed metabolite, the data may be utilized favourably. The available preformed metabolite data may be wisely incorporated into a combined PBPK model of the precursor-metabolite to improve the predictions on metabolite behavior resulting from drug administration. This kind of strategy is utilized frequently in risk assessment. The administration of a metabolite, iv or po, had aided in the modeling and prediction of the formation of toxic metabolites as well as targeted toxicity outcomes. Examples of these elegant works include modeling of the metabolism of styrene oxide from styrene on respiratory tract toxicity (Sarangapani et al., 2002), the metabolism and enterohepatic circulation of di-n-butylphthalate to the monobuytlphate and the glucuronide, compounds that cause impairment of male reproductive tissues (Clewell et al., 2008), the metabolism and oral absorption and of atrazine on toxicity of the pituitary axis and enzyme inhibition (McMullin et al., 2007), the metabolism-associated toxicities of trichloroethylenes (Dobrev et al., 2002), the bioactivation of vinyl chloride to the DNA-reactive epoxide (Chen and Blancato et al., 1989; Reitz et al., 1996; Clewell, 2001), and the inhalation toxicity of acrylate ester (Frederick et al., 1998; 2002; Sweeney et al., 2004). The in vitro/in vivo drug and

Downloaded from dmd.aspetjournals.org at ASPET Journals on April 10, 2024

DMD Fast Forward. Published on October 23, 2008 as DOI: 10.1124/dmd.108.022483
This article has not been copyedited and formatted. The final version may differ from this version.

metabolite transport/distribution and elimination behavior, especially in target organs, should be studied to add to the robustness of the PBPK model. Recently, involvement of Mrp1 in the efflux of rusovastatin in muscle, the target organ for rhadomyolosis has been implied as a plausible cause of toxicity of the statin (Dorajoo et al., 2008); similar transporters of metabolites may need to be identified in toxicity evaluations. Through the refinement of modeling approaches by the incorporation of transporter, enzyme, and modeling approaches, a better solution may be on hand for metabolite toxicity testing.

Downloaded from dmd.aspetjournals.org at ASPET Journals on April 10, 2024

DMD Fast Forward. Published on October 23, 2008 as DOI: 10.1124/dmd.108.022483
This article has not been copyedited and formatted. The final version may differ from this version.

References

Baillie TA, Cayen MN, Founda H, Gerson RJ, Green JD, Grossman SJ, Klunk LJ, LeBlanc B, Perkins DG, and Shipley LA (2002) Contemporary issues in toxicology. Drug metabolites in safety testing. *Toxicol Appl Pharmacol* **182**:188-196

Chen J and Pang KS (1997) Effect of flow on first-pass metabolism of drugs: single pass studies on 4-methylumbelliferone (4MU) conjugation in the serially perfused rat intestine and liver preparations. *J Pharmacol Exp Ther* **280**:24-31.

Clewell HJ, Gentry PR, Gearhart JM, Allen BC, and Andersen ME (2001) Comparison of cancer risk estimates for vinyl chloride using animal and human data with a PBPK model. *Sci Total Environ* **274**:37-66.

Clewell RA, Kremer JJ, Williams CC, Campbell JL, Jr, Andersen ME, and Borghoff SJ (2008) Tissue exposure to free and glucuronidated monobutylphthalate in the pregnant and fetal rat following exposure to di-n-butylphthalate: evaluation with a PBPK model. *Toxicol Sci* **103**:241-259.

Cong D, Doherty M, and Pang KS (2000) A new physiologically-based segregated flow model to explain route-dependent intestinal metabolism. *Drug Metab Dispos* **28**:224-235.

Davis-Bruno KL, and Atrakachi A (2006) A regulatory perspective on issues and approaches in characterizing human metabolites. *Chem Res Toxicol* **19**:1561-1563.

de Lannoy IAM and Pang KS (1993) Combined recirculation of the rat liver and kidney: Studies with enalapril and enalaprilat. *J Pharmacokinet Biopharm* **21**:423-456.

de Lannoy IAM, Barker F 3rd, and Pang KS (1993) Formed and preformed metabolite excretion clearances in liver, a metabolite formation organ: studies on enalapril and enalaprilat in the single-pass and recirculating perfused rat liver. *J Pharmacokinet Biopharm* **21**:395-422.

Dobrev ID, Andersen ME, and Yang RS (2002) In silico toxicology: simulating interaction thresholds for human exposure to mixtures of trichloroethylene, tetrachloroethylene, and 1,1,1-trichloroethane. *Environ Health Perspect* **110**:1031-1039.

Doherty M and Pang KS (2000) Route-dependent metabolism of morphine in the vascularly perfused rat small intestine preparation. *Pharm Res* **17**:291-298.

Dorajoo R, Pereira BP, Yu Z, Gopalakrishnakone P, Leong CC, Wee A, and Lee E (2008) Role of multi-drug resistance associated protein-1 transporter in statin-induced myopathy. *Life Sci* **82**:823-830.

FDA Guidance for Industry. Saftey Testing of Drug Metabolites. February 2008 Pharmacology and Toxicology. http://www.fda.gov/cder/guidance/

Frederick CB, Bush ML, Lomax LG, Black KA, Finch L, Kimbell JS, Morgan KT, Subramaniam RP, Morris JB, and Ultman JS (1998) Application of a hybrid computational fluid dynamics and physiologically based inhalation model for interspecies dosimetry extrapolation of acidic vapors in the upper airways. *Toxicol Appl Pharmacol* **152**:211-231.

Frederick CB, Lomax LG, Black KA, Finch L, Scribner HE, Kimbell JS, Morgan KT, Subramaniam RP, and Morris JB (2002) Use of a hybrid computational fluid dynamics and

Downloaded from dmd.aspetjournals.org at ASPET Journals on April 10, 2024

DMD Fast Forward. Published on October 23, 2008 as DOI: 10.1124/dmd.108.022483
This article has not been copyedited and formatted. The final version may differ from this version.

physiologically based inhalation model for interspecies dosimetry comparisons of ester vapors. *Toxicol Appl Pharmacol* **183**:23-40.

Geng W and Pang KS (1999) Differences in excretion of hippurate, as a metabolite of benzoate and as an administered species in the single pass isolated perfused rat kidney explained. *J Pharmacol Exp Ther* **288**:597-606.

Hastings KL, El-Hage J, Jacobs A, Leighton J, Morse D, and Osterberg RE (2003) Letter to the editor *Toxicol Appl Pharmacol* **190**:91-92.

Humphreys WG and Unger SE (2006) Safety assessment of drug metabolites: Characterization of chemically stable metabolites. *Chem Res Toxicol* **19**:1564-1569.

Johansson F, Allkvist A, Erixon K, Malmvärn A, Nilsson R, Bergman A, Helleday T, and Jenssen D (2004) Screening for genotoxicity using the DRAG assay: investigation of halogenated environmental contaminants. *Mutat Res* **563**:35-47.

Jones DR, Ekins S, Li L, and Hall SD (2007) Computational approaches that predict metabolic intermediate complex formation with CYP3A4 (+b5). *Drug Metab Dispos* **35**:1466-1475.

Khetani SR and Bhatia SN (2006) Engineering tissues for in vitro applications. *Curr Opin Biotechnol* **17**:524-531.

Kothare PA and Zimmerman CL (2002) Intestinal metabolism: the role of enzyme localization in phenol metabolite kinetics. *Drug Metab Dispos* **30**:586-594.

Leeder JS, Dosch HM, Harper PA, Lam P, and Spielberg SP (1989) Fluorescence-based viability assay for studies of reactive drug intermediates. *Anal Biochem* **177**:364-372.

Lee M-Y and Dordick JS (2006) High-throughput human metabolism and toxicity analysis. *Curr Opin Biotechnol* **17**:619-627.

Li AP (2007) Human-based in vitro experimental systems for the evaluation of human drug safety. *Curr Drug Saf* **2**:193-199.

McMullin TS, Hanneman WH, Crammer BK, Tessari JD, and Andersen ME (2007) Oral absorption and oxidative metabolism of atrazine in rats evaluated by physiological modeling approaches. *Toxicology* **240**:1-14.

Naito S, Furuta S, Yoshida T, Kitada m, Fueki O, Unno T, Ohno Y, Onodera H, Kawamura N, Kurokawa M, Sagami F, Shinoda K, Nakazawa T, and Yamaaki T (2007) Current opinion: Safety evaluation of drug metabolites in development of pharmaceutics. *J Toxicol Sci* **32**:329-341.

Pang KS (2003) Modeling of intestinal drug absorption. Roles of transporters and metabolic enzymes (for the Gillette Series). *Drug Metab Dispos* **31**:1507-1519.

Pang KS and Chiba M (1994) Metabolism: Scaling up from *in vitro* to organ and whole body, in *Handbook of Experimental Pharmacology* (P. G. Welling and L.P. Balant eds) pp 101-187, Springer-Verlag, Stuttgart.

Pang KS, Morris ME, and Sun H (2008) Formed and preformed metabolites: facts and comparisons. *J Pharm Pharmacol* **60**:1247-1275.

Downloaded from dmd.aspetjournals.org at ASPET Journals on April 10, 2024

DMD Fast Forward. Published on October 23, 2008 as DOI: 10.1124/dmd.108.022483
This article has not been copyedited and formatted. The final version may differ from this version.

Prueksaritanont T, Lin JH, and Baillie TA (2006) Complicating factors in safety testing of drug kinetics: Kinetic differences between generated and preformed metabolites. *Toxicol Appl Pharmacol* **217**:143-152

Retiz RH, Gargas ML, Andersen ME, Provan WM, and Green TL (1996) Predicting cancer risk from vinyl chloride exposure with a physiologically based pharmacokinetic model. *Toxicol Appl Pharmacol* **137**:253-267.

Sarangapani R, Teeguarden JG, Cruzan G, Clewell HJ, and Andersen ME (2002) Physiologically based pharmacokinetic modelling of styrene and styrene oxide respiratory-tract dosimetry in rodents and humans. *Inhal Toxicol* **14**:789-834.

Smith DA and Obach RS (2005) Seeing through the MIST: abundance versus percentage. Commentary on metabolite in safety testing. *Drug Metab Dispos* **33**:1409-1417.

Smith DA and Obach RS (2006) Metabolites and safety: What are the concerns, and how should we address them? *Chem Res Toxicol* **19**:1570-1579.

Stevens JL (2006) Future of toxicology - Mechanisms of toxicity and drug safety: where do we go from here? *Chem Res Toxicol* **19**:1393-1401.

Sweeney LM, Andersen ME, and Gargas ML (2004) Ethyl acrylate risk assessment with a hybrid computational fluid dynamics and physiologically based nasal dosimetry model. *Toxicol Sci* **79**:394-403.

Tam D, Tirona RG, and Pang KS (2003) Segmental intestinal transporters and metabolic enzymes on intestinal drug absorption. *Drug Metab Dispos* **31**:373-383.

Tan E, Lu T, and Pang KS (2001) Futile cycling of estrone sulfate and estrone in the recirculating, perfused rat liver. *J Pharmacol. Exp Ther* **297**: 423-436.

Yang J, Jamei M, Yeo KR, Tucker GT, and Rostami-Hodjegan A (2007) Prediction of intestinal first-pass drug metabolism. *Curr Drug Metab* **8**:676-684.

Xu X, Tang BK, and Pang KS (1990) Sequential metabolism of salicylamide exclusively to gentisamide 5-glucuronide and not gentisamide sulfate conjugates in single-pass in situ perfused rat liver. *J Pharmacol Exp Ther* **253**:965-973.

Downloaded from dmd.aspetjournals.org at ASPET Journals on April 10, 2024

DMD Fast Forward. Published on October 23, 2008 as DOI: 10.1124/dmd.108.022483
This article has not been copyedited and formatted. The final version may differ from this version.

Footnotes

This work was supported by the Canadian Institutes for Health Research.

Downloaded from dmd.aspetjournals.org at ASPET Journals on April 10, 2024

DMD Fast Forward. Published on October 23, 2008 as DOI: 10.1124/dmd.108.022483
This article has not been copyedited and formatted. The final version may differ from this version.

Legends

Figure 1. Schematic depiction of drug (D) and metabolite (M) behaviors in the TM (A) and SFM (B). For TM, the intestinal blood (Q_I) perfuses the entire intestinal tissue, the site of metabolism and absorption from the lumen. For SFM, intestinal blood is segregated to perfuse the non-metabolizing (Q_s) and enterocyte-mucosal (Q_{en}) regions. For the oral route of administration, the entire oral dose passes through the enterocyte region for both TM and SFM. For intravenous or systemically delivered species, the total flow (Q_I) perfused the intestine tissue and enterocyte region for TM, but there is only partial flow (Q_{en}) reaching the enterocyte region for the SFM. The drug equilibrates with those in the corresponding tissue layers with intrinsic transfer clearances CL_{d1} and CL_{d2} for TM, or CL_{d1} and CL_{d2}, CL_{d3} and CL_{d4} for SFM. Subscripts enb, en, sb, and s denote enterocyte blood, enterocyte region, serosal blood and serosal region, respectively. The absorptive, metabolic and efflux activities within the villus tips of the mucosal layer are represented by the rate constant, k_a, and metabolic and secretory intrinsic clearances, $CL_{int,met,I}$ and $CL_{int,sec,I}$, respectively. Gastrointestinal transit or degradation rate constant in the lumen is denoted by k_g. A similar set of parameters exist for the metabolite, qualified by {mi}.

Figure 2. The area under the curve of the preformed metabolite after systemic administration, AUC_{iv}{pmi}, for the TM (A,C) and SFM (B,D) against the $CL_{int,met,I}${mi} and $CL_{int,sec,I}${mi} for CL_{d1}{mi}=CL_{d2}{mi}= 2 ml/min (A,B) or 0.01 ml/min (C,D). The AUC_{iv}{pmi} for TM was lower than that for SFM because of the flow terms, Q_I for the TM and Q_{en} for the SFM (Eqs. 1 and 2). Note that AUC_{iv}{pmi} was strongly modulated by $CL_{int,met,I}${mi} and not $CL_{int,sec,I}${mi}. For this simulation, CL_{d2}{mi} was set as identical to CL_{d1}{mi}, i.e., CL_{d2}{mi}/CL_{d1}{mi} = 1.

Figure 3. The area under the curve of the preformed metabolite after systemic administration, AUC_{iv}{pmi}, for the TM (A,C) and SFM (B,D) against $CL_{int,sec,I}${mi} and k_a{mi} for CL_{d1}{mi} = CL_{d2}{mi} = 2 ml/min (A,B) or 0.01 ml/min (C,D). The effects of $CL_{int,sec,I}${mi} were neutralized by k_a{mi}. For this simulation, CL_{d2}{mi} was set as identical to CL_{d1}{mi},or CL_{d2}{mi/CL_{d1}{mi} = 1.

Figure 4. The area under the curve of the preformed metabolite after oral administration, AUC_{po}{pmi}, same for the TM and SFM. (A) The influence of $CL_{int,sec,I}${mi} was much less than those of $CL_{int,met,I}${mi}; (B) the effects of $CL_{int,sec,I}${mi} was neutralized by k_a{mi}; (C) AUC_{po}{pmi} was affected directly by the ratio of CL_{d2}{mi}/CL_{d1}{mi}.

Figure 5. The systemic availability F{pmi}, given by AUC_{po}{pmi}/AUC_{iv}{pmi}, for the TM (A,C) and SFM (B,D) against the $CL_{int,met,I}${mi} and $CL_{int,sec,I}${mi} for CL_{d1}{mi} = CL_{d2}{mi} = 2 ml/min (A,B) or 0.01 ml/min or (C,D). The F{pmi} for TM was higher than that for SFM because of the flow terms, Q_I for the TM and Q_{en} for the SFM (Eqs. 1 and 2). Note that AUC_{iv}{pmi} was strongly modulated by $CL_{int,met,I}${mi} and not $CL_{int,sec,I}${mi}. For this simulation, CL_{d2}{mi} was set as identical to CL_{d1}{mi}, i.e., CL_{d2}{mi}/CL_{d1}{mi} = 1.

Figure 6. Dependence of the areas under the curve of the formed metabolite on precursor parameters: when the precursor was given iv [AUC_{iv}{mi,P}, (A,C)] and po [AUC_{po}{mi,P}, (B,D)]: against precursor $CL_{int,met,I}$ and $CL_{int,sec,I}$ (A,B) and $CL_{int,sec,I}$ and k_a (C,D), when CL_{d1}{mi} equaled CL_{d2}{mi}. The AUC_{iv}{mi,P} and AUC_{po}{mi,P} were identical for the TM

Downloaded from dmd.aspetjournals.org at ASPET Journals on April 10, 2024

DMD Fast Forward. Published on October 23, 2008 as DOI: 10.1124/dmd.108.022483
This article has not been copyedited and formatted. The final version may differ from this version.

and SFM (Eqs. 4 and 5). Note that there was a strong influence of $CL_{int,sec,I}$ and $CL_{int,met,I}$ on the AUCs of the formed metabolites, and that increasing k_a values neutralized the effect of luminal secretion of the precursor.

Figure 7. Dependence of the areas under the curve of the formed metabolite on metabolite parameters: when drug was given iv [AUC_{iv}{mi,P}, (A,C)] and po [AUC_{po}{mi,P},(B,D)]: against the $CL_{int,sec,I}${mi} and $CL_{int,met,I}${mi} when CL_{d2}{mi/CL_{d1}{mi}= 1 (A,B), and CL_{d2}{mi/CL_{d1}{mi} and k_a{mi} (C,D) of the metabolite. Note that increasing k_a{mi}neutralized the effect of luminal secretion of the precursor.

Figure 8. Simulation of the time courses of preformed metabolite (profiles) for Cases 1 and 2 (Table 1): CL_d{mi} = 2 ml/min (A), or 0.01 ml/min (B), with doses of 100 units for the preformed metabolite; k_a{mi} = 0.05 min^{-1}; reservoir and lumen volumes of 200 and 2 ml, respectively. The initial concentration of preformed metabolite in the dosing compartment (reservoir) is 0.5(dose unit/ml) for the iv cases and 50 (dose unit/ml) in the intestinal lumen for po cases. Other parameters of the preformed metabolite used for simulation were shown in Table 1. (A) The graphs differed for CL_d{mi} = 2 ml/min (A) and CL_d{mi} = 0.01 ml/min (B). At high CL_d{mi}, the $t_{1/2}$ for the TM (iv and po) was faster than that for the SFM (iv and po) (A) At low CL_d{mi}, the graphs were identical for TM and SFM after iv or po dosing of the preformed metabolite (B).

Figure 9. Simulation of the time courses of formed metabolite (profiles) for Cases 1 and 2 (Table 1): CL_d{mi} = 2 ml/min for Case 1A (A) and Case 1B (B); and CL_d{mi} = 0.01 ml/min for Case 2A (C) and Case 2B (D), and k_a{mi} = 0.05 min^{-1}, with doses of 100 units for precursor. Since the reservoir and lumen volumes were 200 and 2 ml, respectively, the initial concentration of precursor in dosing compartment is 0.5 (dose unit/ml) in reservoir for the iv cases and 50(dose unit/ml) in intestinal lumen for po cases. Other parameters of precursor and metabolite used for simulation were shown in Table 1. The metabolite curves were different for k_a = 0.01 min^{-1} (A) and (C) vs. k_a = 1 min^{-1} (B) and (D). Higher (formed) metabolite levels were observed with higher k_a and higher CL_d{mi}. The absorptive constant, k_a, also influenced the time course/profile of the formed metabolite by reducing the effective secretion intrinsic clearance ($CL_{int,sec,I}$), thereby increasing the rate of drug metabolism.

Figure 10. Simulation of the time courses of formed metabolite (profiles) for Cases 1 and 2 (similar to those of Figure 9). CL_d{mi} = 2 ml/min for Case 1A (A) and Case 1B (B), and CL_d{mi} = 0.01 ml/min for Case 2A (C) and Case 2B (D); and k_a{mi} = 0.05 (dose unit/ml). The precursor dose of 100 units was used, whereas the dose of the preformed metabolite was estimated with Eq. 8, such that AUC_{po}{mi,P} = AUC_{po}{pmi}. Note again that higher levels of the metabolites were observed with higher k_a and higher CL_d{mi}. The concentration profiles of the preformed metabolite were consistently higher than those of the formed metabolite for the TM or SFM, especially at the earlier time points, although the areas under the curve of the preformed and formed metabolites were identical.

Downloaded from dmd.aspetjournals.org at ASPET Journals on April 10, 2024

DMD Fast Forward. Published on October 23, 2008 as DOI: 10.1124/dmd.108.022483
This article has not been copyedited and formatted. The final version may differ from this version.

Table1: Parameters for the simulation of time-courses of preformed and formed metabolites with the TM and SFM (for simulating Figs. 8 and 9)

Parameters	**Case 1**	**Case 2**
Drug		
CL_{d1} (ml/min)	2	2
CL_{d2} (ml/min)	2	2
CL_{d3} (ml/min)	2	2
CL_{d4} (ml/min)	2	2
k_a (min^{-1})[a]	0.01 & 1	0.01 & 1
k_g (min^{-1})	0.01	0.01
$CL_{int,sec,I}$ (ml/min)	0.5	0.5
$CL_{int,met,I}$ (ml/min)	0.5	0.5
Metabolite		
CL_{d1}{mi} (ml/min)	2	0.01
CL_{d2}{mi} (ml/min)	2	0.01
CL_{d3}{mi} (ml/min)	2	0.01
CL_{d4}{mi} (ml/min)	2	0.01
k_a{mi} (min^{-1})	0.05	0.05
k_g{mi} (min^{-1})	0.01	0.01
$CL_{int,sec,I}${mi} (ml/min)	0.5	0.5
$CL_{int,met,I}${mi} (ml/min)	0.5	0.5
k_g{mi} (min^{-1})	0.01	0.01

[a] k_a of 0.01 and 1 min^{-1} corresponded to conditions A and B respectively.

Downloaded from dmd.aspetjournals.org at ASPET Journals on April 10, 2024

Table 2. Ratios of the areas under the curve for the preformed {pmi}and formed {mi,P} metabolites according to the Traditional Model (TM) and Segregated Flow Model (SFM)

Parameter	Equations
TM $\frac{\mathrm{AUC_{iv}\{mi,P\}}}{\mathrm{AUC_{iv}\{pmi\}}}$	$\frac{Dose_{iv}Q_I CL_{\mathrm{int},met,I} CL_{d2}\{mi\}}{Dose_{iv}\{pmi\}\left((1-F_{abs})CL_{\mathrm{int,sec},I}+CL_{\mathrm{int},met,I}\right)\left((1-F_{abs}\{mi\})CL_{\mathrm{int,sec},I}\{mi\}\left[CL_{d1}\{mi\}+Q_I\right]+Q_I\left[CL_{d2}\{mi\}+CL_{\mathrm{int},met,I}\{mi\}\right]+CL_{d1}\{mi\}CL_{\mathrm{int},met,I}\{mi\}\right)}$
SFM $\frac{\mathrm{AUC_{iv}\{mi,P\}}}{\mathrm{AUC_{iv}\{pmi\}}}$	$\frac{Dose_{iv}Q_{en} CL_{\mathrm{int},met,I} CL_{d2}\{mi\}}{Dose_{iv}\{pmi\}\left((1-F_{abs})CL_{\mathrm{int,sec},I}+CL_{\mathrm{int},met,I}\right)\left((1-F_{abs}\{mi\})CL_{\mathrm{int,sec},I}\{mi\}\left(CL_{d1}\{mi\}+Q_{en}\right)+Q_{en}\left(CL_{d2}\{mi\}+CL_{\mathrm{int},met,I}\{mi\}\right)+CL_{d1}\{mi\}CL_{\mathrm{int},met,I}\{mi\}\right)}$
TM & SFM $\frac{\mathrm{AUC_{po}\{mi,P\}}}{\mathrm{AUC_{po}\{pmi\}}}$	$\frac{Dose_{po}F_{abs}CL_{\mathrm{int},met,I}}{Dose_{po}\{pmi\}F_{abs}\{mi\}\left[(1-F_{abs})CL_{\mathrm{int,sec},I}+CL_{\mathrm{int},met,I}\right]}$
TM $\frac{\mathrm{AUC_{po}\{pmi\}}}{\mathrm{AUC_{iv}\{pmi\}}}$	$\frac{F_{abs}\{mi\}Dose_{po}\{pmi\}Q_I CL_{d2}\{mi\}}{Dose_{iv}\{pmi\}\left[\left(1-F_{abs}\{mi\}\right)CL_{\mathrm{int,sec},I}\{mi\}\left(Q_I+CL_{d1}\{mi\}\right)+Q_I\left(CL_{d2}\{mi\}+CL_{\mathrm{int},met,I}\{mi\}\right)+CL_{d1}\{mi\}CL_{\mathrm{int},met,I}\{mi\}\right]}$
SFM $\frac{\mathrm{AUC_{po}\{pmi\}}}{\mathrm{AUC_{iv}\{pmi\}}}$	$\frac{F_{abs}\{mi\}Dose_{po}\{pmi\}Q_{en} CL_{d2}\{mi\}}{Dose_{iv}\{pmi\}\left[\left(1-F_{abs}\{mi\}\right)CL_{\mathrm{int,sec},I}\{mi\}\left(Q_{en}+CL_{d1}\{mi\}\right)+Q_{en}\left(CL_{d2}\{mi\}+CL_{\mathrm{int},met,I}\{mi\}\right)+CL_{d1}\{mi\}CL_{\mathrm{int},met,I}\{mi\}\right]}$
TM & SFM $\frac{\mathrm{AUC_{po}\{mi,P\}}}{\mathrm{AUC_{iv}\{mi,P\}}}$	$\frac{F_{abs}Dose_{po}}{Dose_{iv}}$

[a] $F_{abs}=\frac{k_a}{k_a+k_g}$ and $F_{abs}\{mi\}=\frac{k_a\{mi\}}{k_a\{mi\}+k_g\{mi\}}$

[b] TM and SFM denote Traditional Model and Segregated Flow Model, respectivel

Downloaded from dmd.aspetjournals.org at ASPET Journals on April 10, 2024

DMD Fast Forward. Published on October 23, 2008 as DOI: 10.1124/dmd.108.022483
This article has not been copyedited and formatted. The final version may differ from this version.

Figure 1

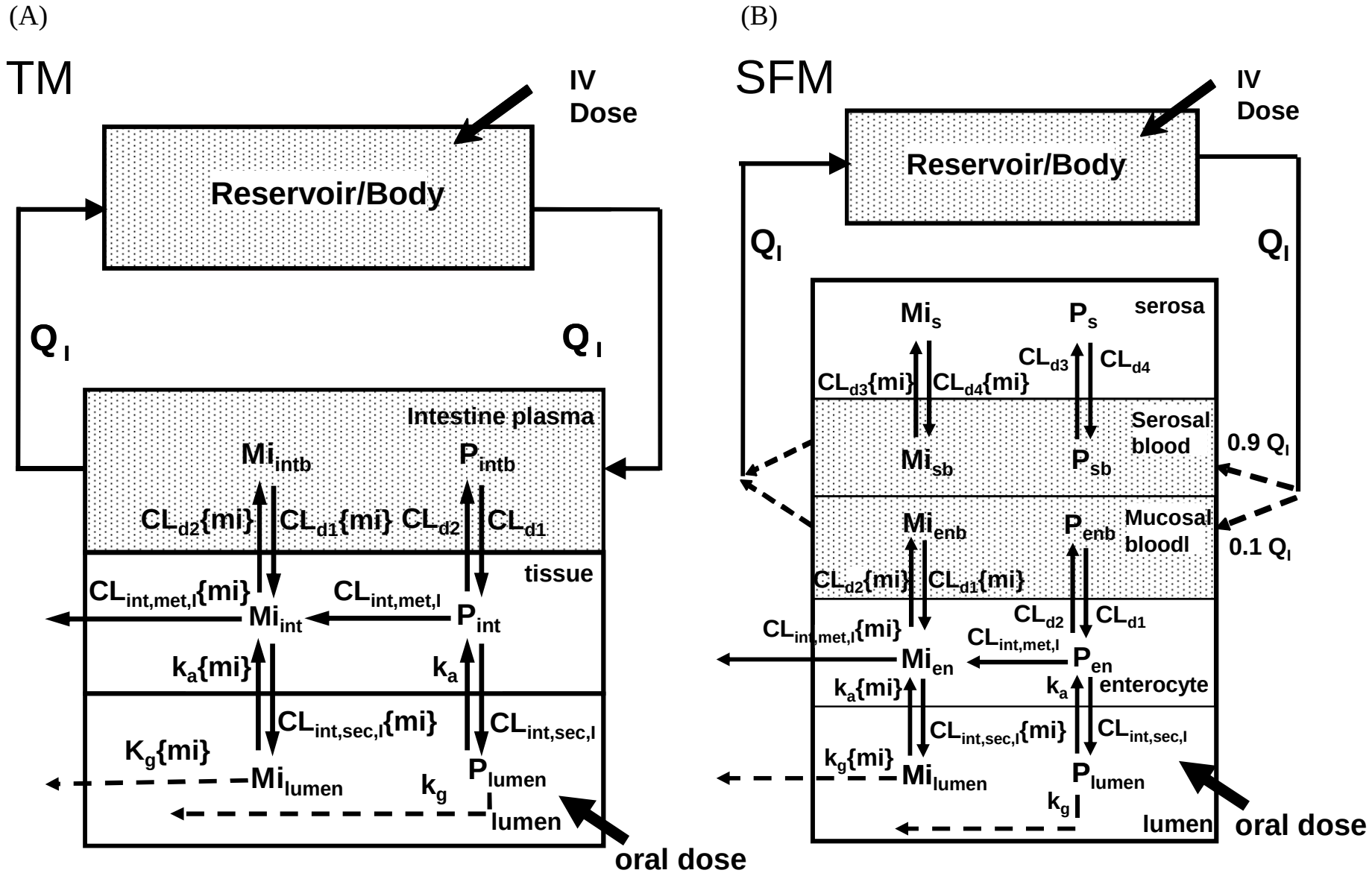

DMD Fast Forward. Published on October 23, 2008 as DOI: 10.1124/dmd.108.022483
This article has not been copyedited and formatted. The final version may differ from this version.

Downloaded from dmd.aspetjournals.org at ASPET Journals on April 10, 2024

Figure 2

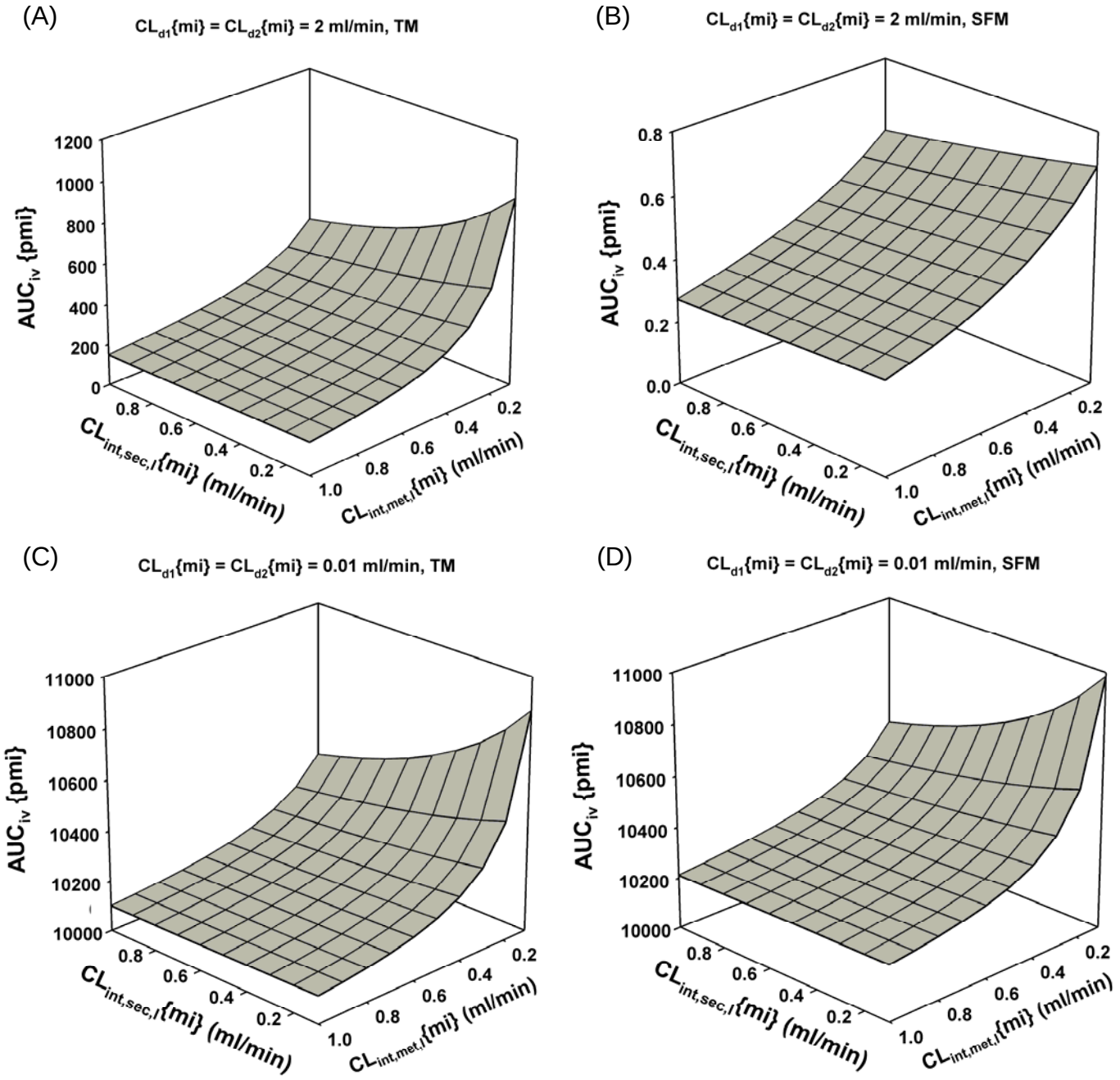

Downloaded from dmd.aspetjournals.org at ASPET Journals on April 10, 2024

DMD Fast Forward. Published on October 23, 2008 as DOI: 10.1124/dmd.108.022483
This article has not been copyedited and formatted. The final version may differ from this version.

Figure 3

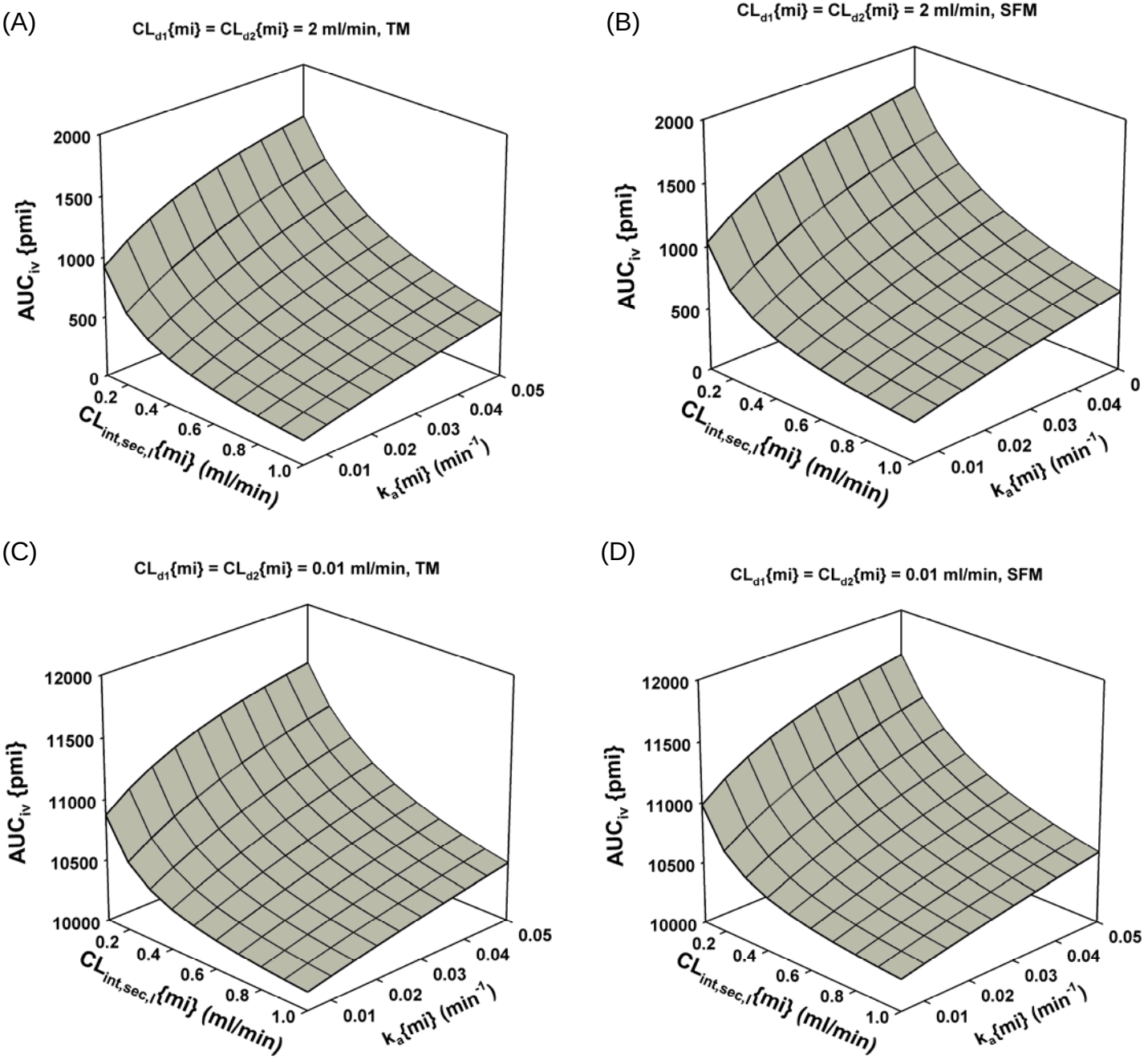

DMD Fast Forward. Published on October 23, 2008 as DOI: 10.1124/dmd.108.022483
This article has not been copyedited and formatted. The final version may differ from this version.

Downloaded from dmd.aspetjournals.org at ASPET Journals on April 10, 2024

DMD Fast Forward. Published on October 23, 2008 as DOI: 10.1124/dmd.108.022483
This article has not been copyedited and formatted. The final version may differ from this version.

Figure 4

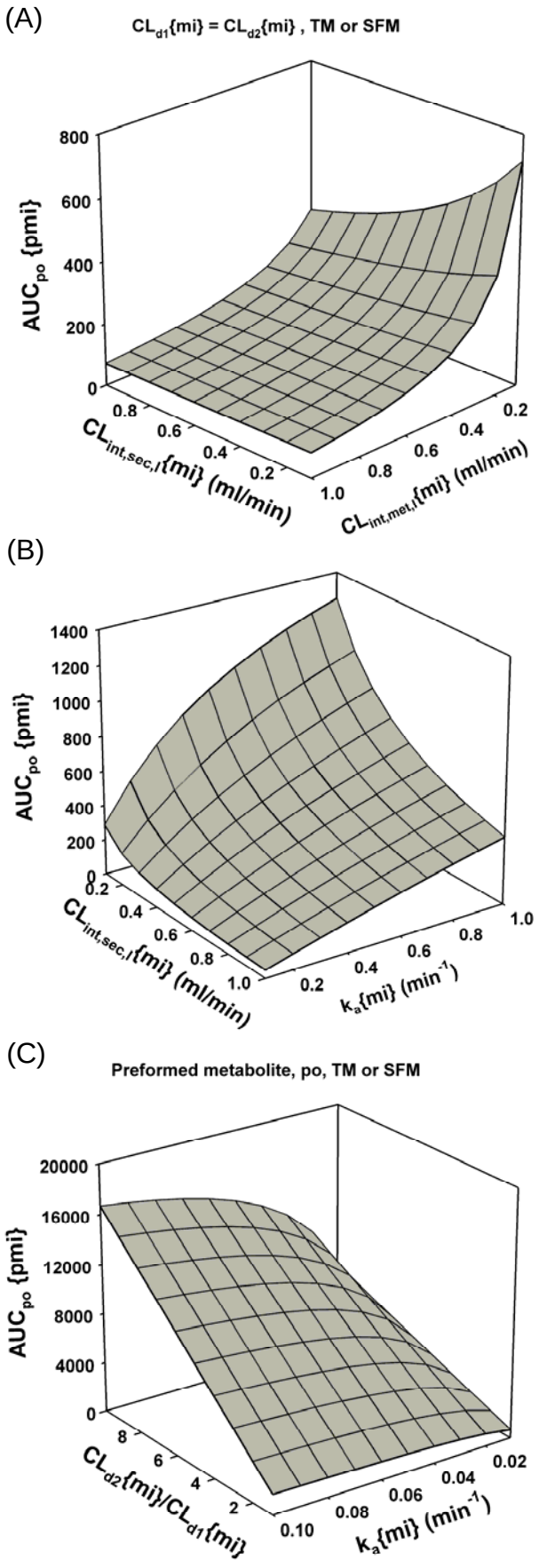

Downloaded from dmd.aspetjournals.org at ASPET Journals on April 10, 2024

Figure 5

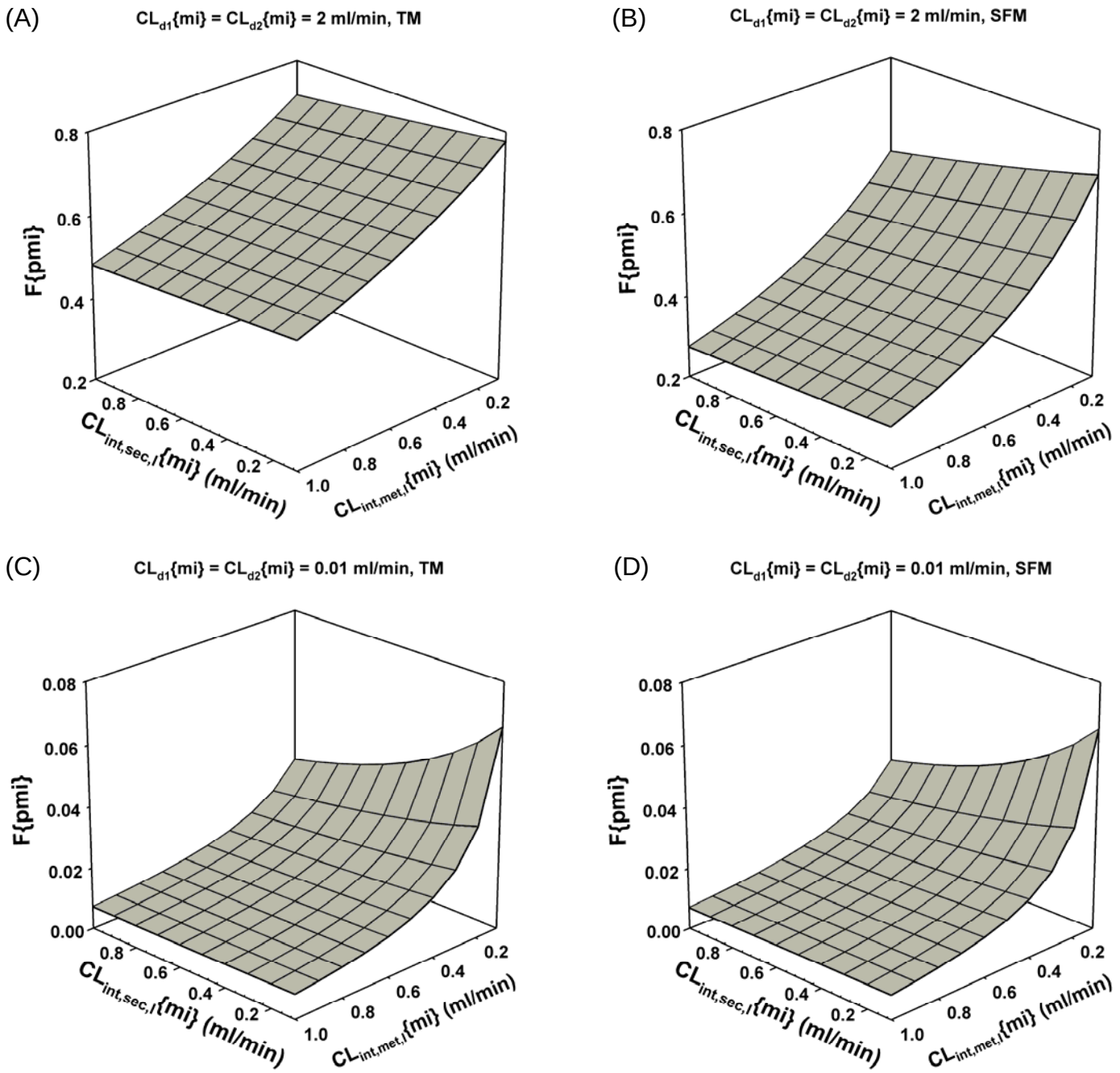

Downloaded from dmd.aspetjournals.org at ASPET Journals on April 10, 2024

DMD Fast Forward. Published on October 23, 2008 as DOI: 10.1124/dmd.108.022483
This article has not been copyedited and formatted. The final version may differ from this version.

Figure 6

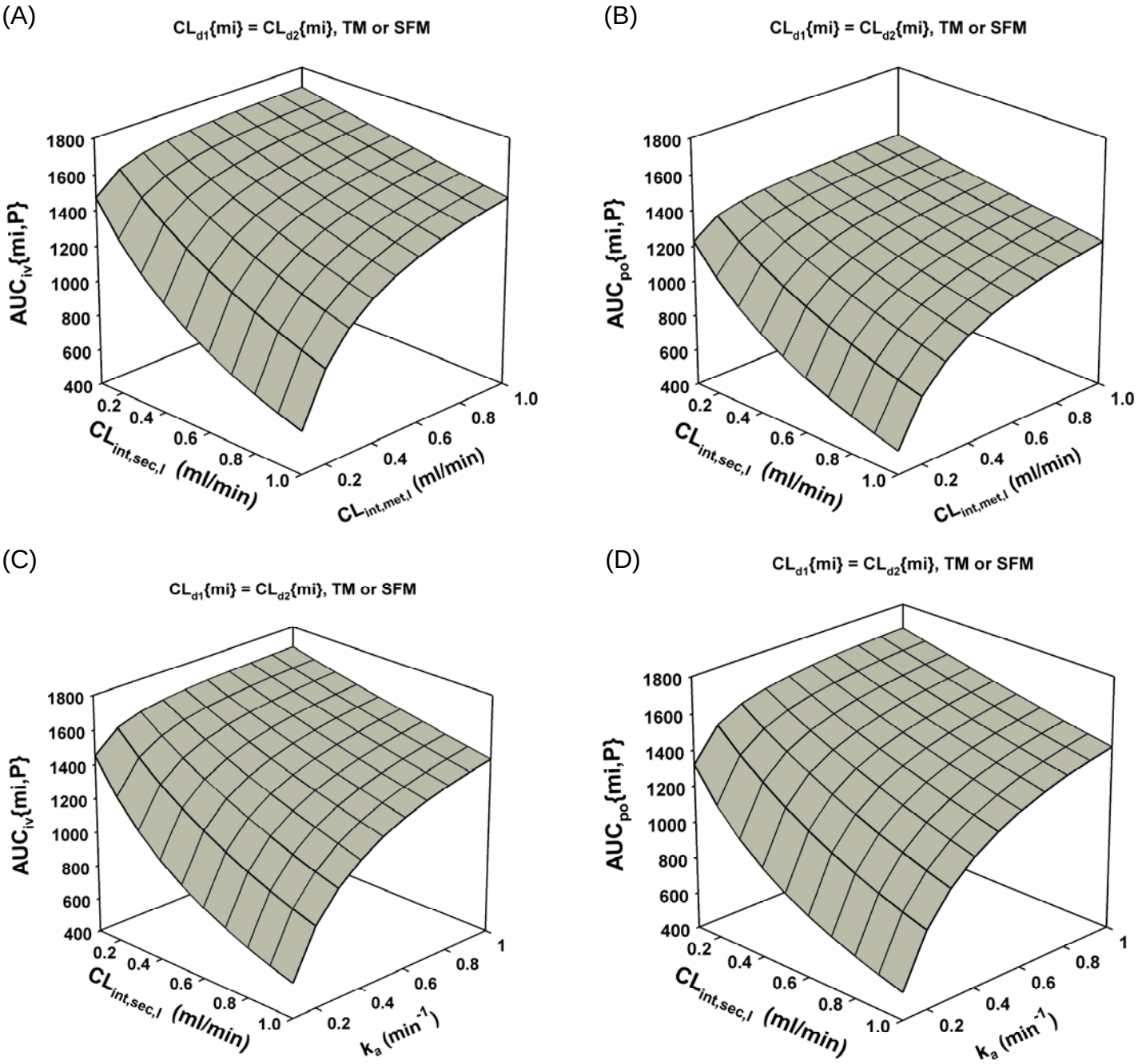

Downloaded from dmd.aspetjournals.org at ASPET Journals on April 10, 2024

DMD Fast Forward. Published on October 23, 2008 as DOI: 10.1124/dmd.108.022483
This article has not been copyedited and formatted. The final version may differ from this version.

Figure 7

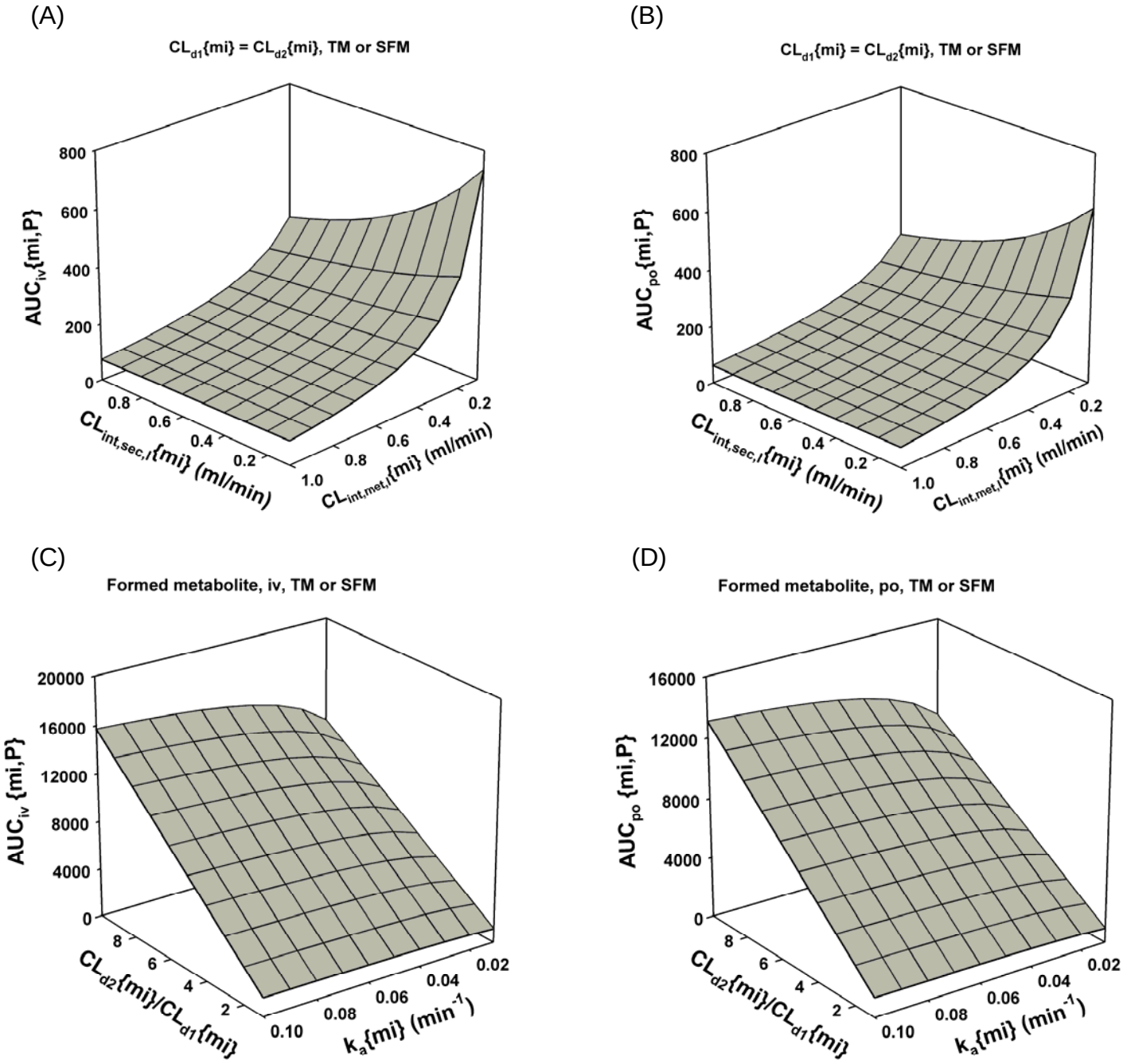

DMD Fast Forward. Published on October 23, 2008 as DOI: 10.1124/dmd.108.022483
This article has not been copyedited and formatted. The final version may differ from this version.

Downloaded from dmd.aspetjournals.org at ASPET Journals on April 10, 2024

Figure 8

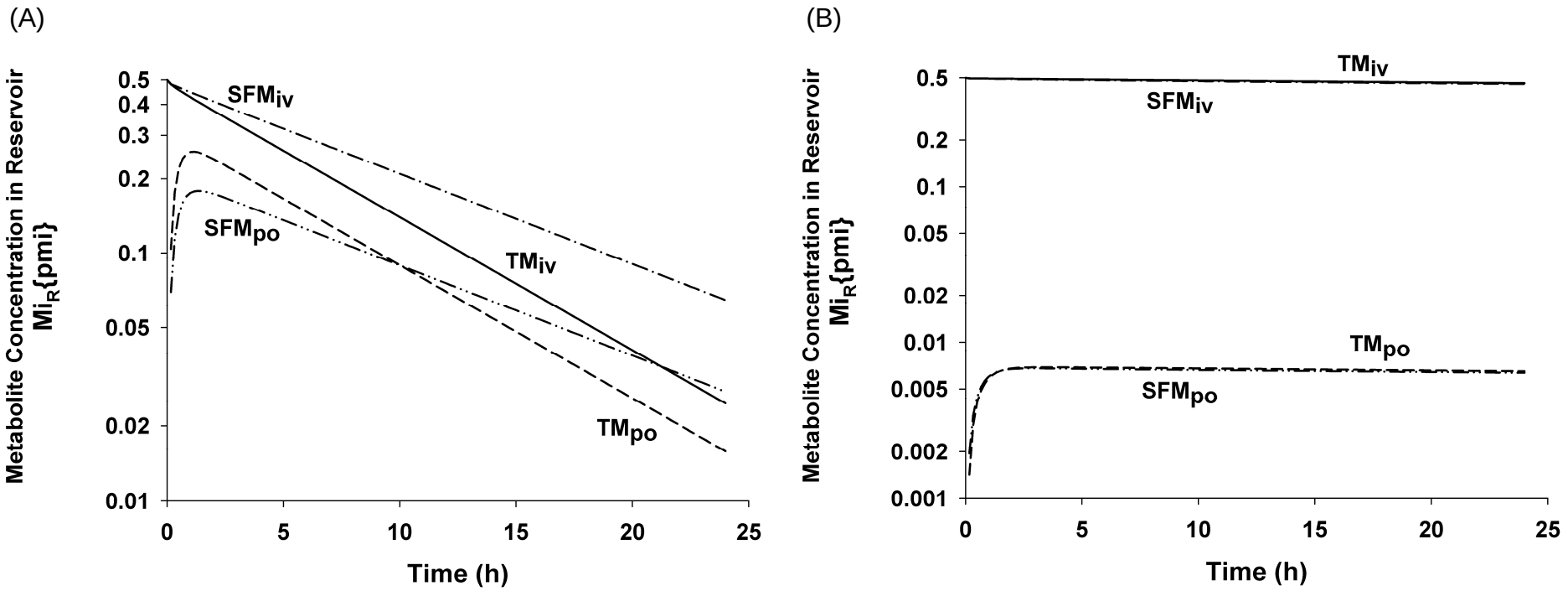

DMD Fast Forward. Published on October 23, 2008 as DOI: 10.1124/dmd.108.022483
This article has not been copyedited and formatted. The final version may differ from this version.

Downloaded from dmd.aspetjournals.org at ASPET Journals on April 10, 2024

Figure 9

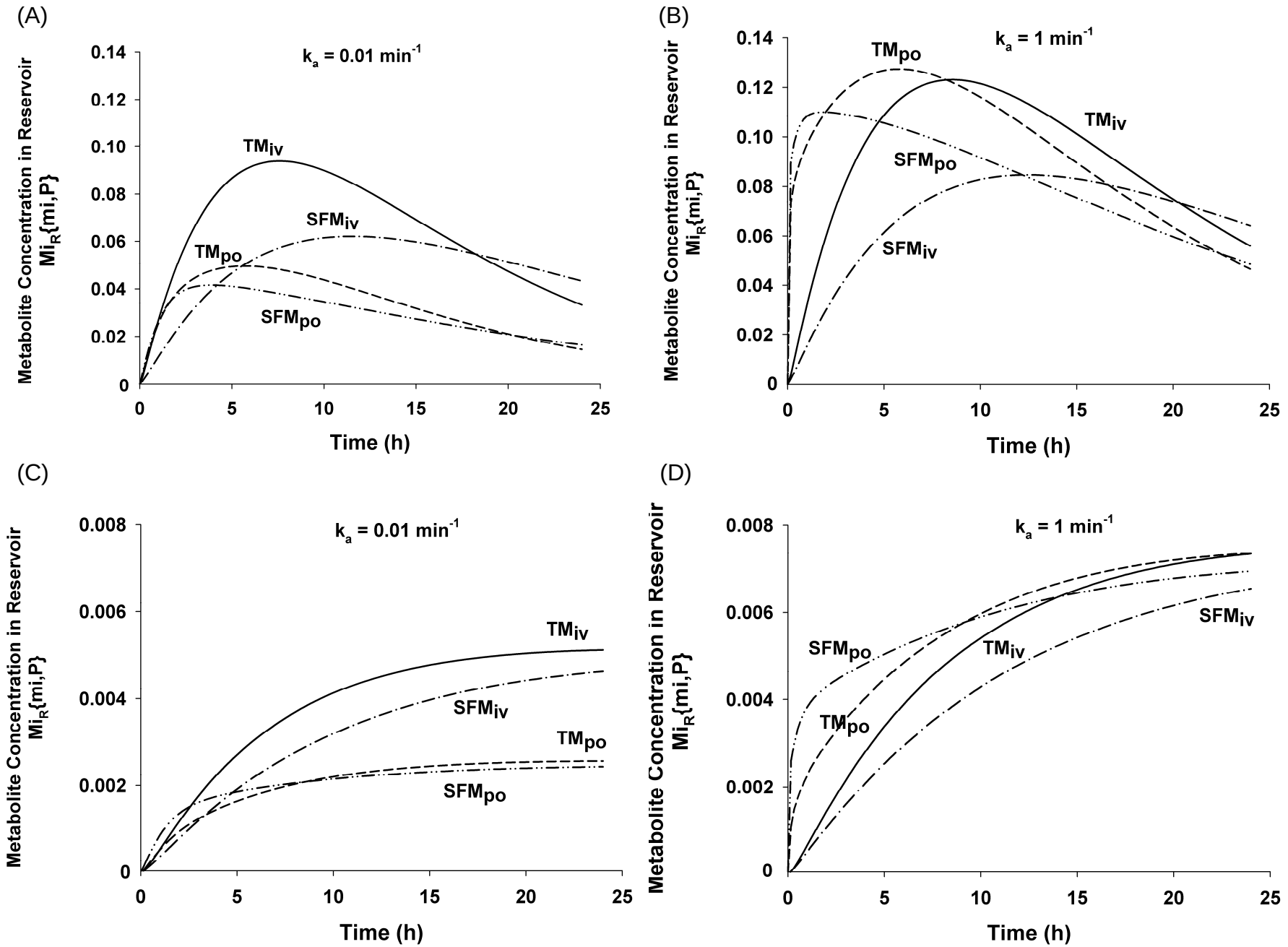

DMD Fast Forward. Published on October 23, 2008 as DOI: 10.1124/dmd.108.022483
This article has not been copyedited and formatted. The final version may differ from this version.

Downloaded from dmd.aspetjournals.org at ASPET Journals on April 10, 2024

Figure 10

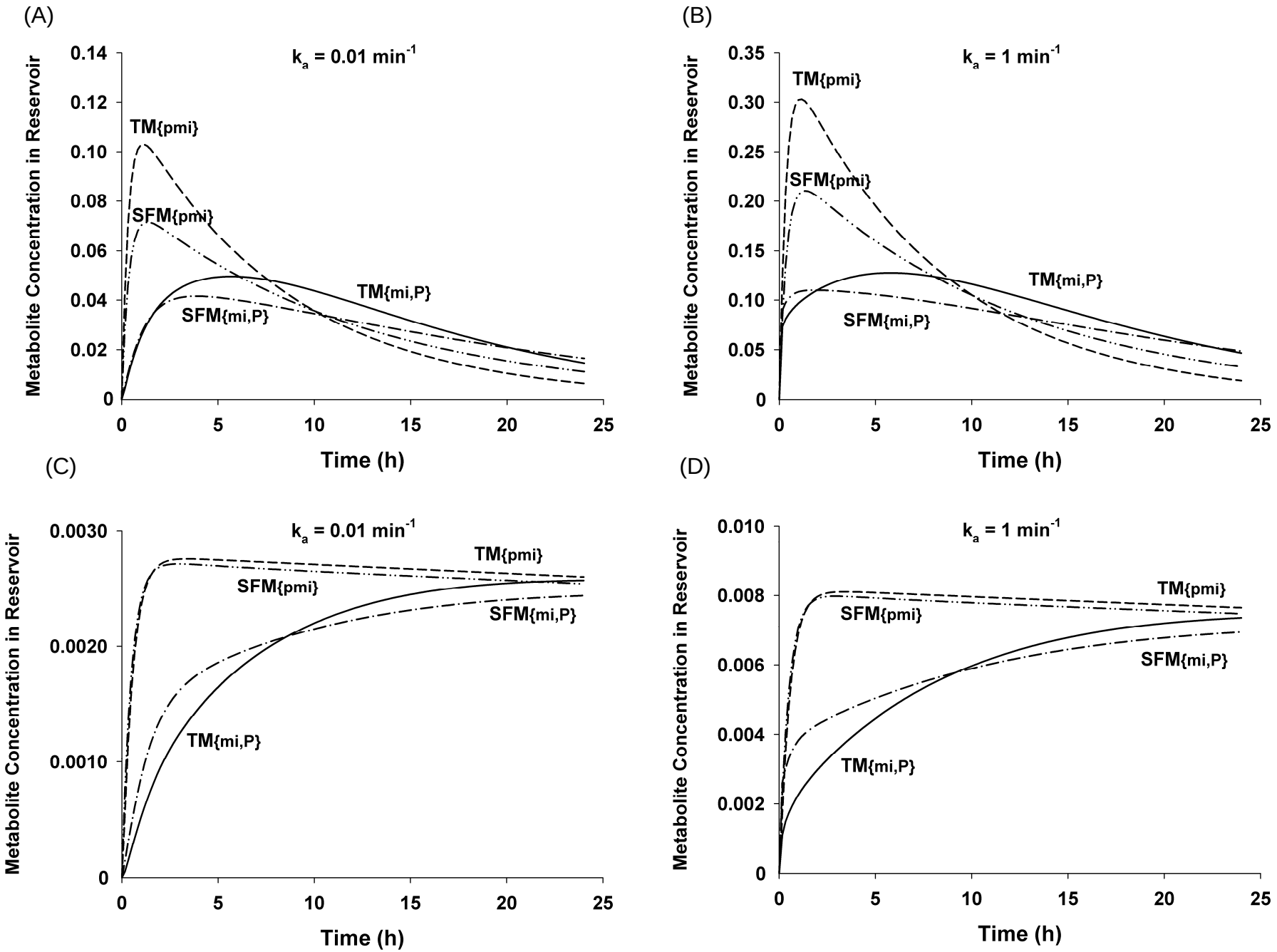

DMD Fast Forward. Published on October 23, 2008 as DOI: 10.1124/dmd.108.022483
This article has not been copyedited and formatted. The final version may differ from this version.

Downloaded from dmd.aspetjournals.org at ASPET Journals on April 10, 2024

DMD Fast Forward. Published on October 23, 2008 as DOI: 10.1124/dmd.108.022483
This article has not been copyedited and formatted. The final version may differ from this version.

Appendix: Mass balance equations and the corresponding matrix for preformed and formed metabolite in TM and SFM model

In the following section, P denotes the concentration of the precursor, whereas Mi denotes the concentration of the metabolite, either preformed ({pmi}) or formed from the administration of the precursor ({mi,P}). V denotes the volume in each compartment, f, the unbound fraction; subscripts: I, R, intb, int, and lumen denote the intestine, reservoir, intestinal blood, intestinal tissue, and intestine lumen, respectively. Subscripts, s, sb, en, and enb, describe the serosal, serosal blood, enterocyte, enterocyte blood, respectively. Q_I describes the total intestinal blood flow rate, or sum of the blood flows perfusing the enterocyte layer (Q_{enb}, 10% of Q_I) and the serosal layer (Q_{sb}, 90% of Q_I). The parameters pertaining to the metabolite are qualified by {mi}. Definition of the kinetic parameters has been given in the Methods Section.

I. TM: preformed metabolite

Rate of change of metabolite in reservoir,

$$V_R \frac{dMi_R}{dt} = Q_I(Mi_{intb} - Mi_R) \quad \text{(A1)}$$

Rate of change of metabolite in intestinal blood,

$$V_{intb} \frac{dMi_{intb}}{dt} = Q_I(Mi_R - Mi_{intb}) + f_L\{mi\}CL_{d2}\{mi\}Mi_{int} - f_b\{mi\}CL_{d1}\{mi\}Mi_{intb} \quad \text{(A2)}$$

Rate of change of metabolite in tissue,

$$V_{int} \frac{dMi_{int}}{dt} = f_b\{mi\}CL_{d1}\{mi\}Mi_{intb} + k_a\{mi\}Mi_{lumen}V_{lumen} - f_L\{mi\}(CL_{d2}\{mi\} + CL_{int,met,I}\{mi\} + CL_{int,sec,I}\{mi\})Mi_{int} \quad \text{(A3)}$$

Rate of change of metabolite in intestine lumen,

$$V_{lumen} \frac{dMi_{lumen}}{dt} = -(k_a\{mi\} + k_g\{mi\})Mi_{lumen}V_{lumen} + f_L\{mi\}CL_{int,sec,I}\{mi\}Mi_{int} \quad \text{(A4)}$$

Downloaded from dmd.aspetjournals.org at ASPET Journals on April 10, 2024

DMD Fast Forward. Published on October 23, 2008 as DOI: 10.1124/dmd.108.022483
This article has not been copyedited and formatted. The final version may differ from this version.

Matrix for the TM model: preformed metabolite

$$\begin{pmatrix} \frac{Q_I}{V_R} & -\frac{Q_I}{V_{intb}} & 0 & 0 \\ -\frac{Q_I}{V_R} & \frac{Q_I + CL_{d1}\{mi\}}{V_{intb}} & -\frac{CL_{d2}\{mi\}}{V_{int}} & 0 \\ 0 & \frac{CL_{d1}\{mi\}}{V_{intb}} & \frac{CL_{int,sec,I}\{mi\} + CL_{int,met,I}\{mi\} + CL_{d2}\{mi\}}{V_{int}} & -k_a\{mi\} \\ 0 & 0 & -\frac{CL_{int,sec,I}\{mi\}}{V_{int}} & k_a\{mi\} + k_g\{mi\} \end{pmatrix}$$

II. TM: Formed metabolite

Rates of change of precursor and metabolite in reservoir,

$$V_R \frac{dP_R}{dt} = Q_I (P_{intb} - P_R) \quad \text{(A5)}$$

$$V_R \frac{dMi_R}{dt} = Q_I (Mi_{intb} - Mi_R) \quad \text{(A6)}$$

Rates of change of precursor and metabolite in intestinal blood,

$$V_{intb} \frac{dP_{intb}}{dt} = Q_I (P_R - P_{intb}) + f_L CL_{d2} P_{int} - f_b CL_{d1} P_{intb} \quad \text{(A7)}$$

$$V_{intb} \frac{dMi_{intb}}{dt} = Q_I (Mi_R - Mi_{intb}) + f_L \{mi\} CL_{d2}\{mi\} Mi_{int} - f_b \{mi\} CL_{d1}\{mi\} Mi_{intb} \quad \text{(A8)}$$

Rates of change of precursor and metabolite in intestine tissue,

$$V_{int} \frac{dP_{int}}{dt} = f_b CL_{d1} P_{intb} + k_a P_{lumen} V_{lumen} - f_L (CL_{d2} + CL_{int,met,I} + CL_{int,sec,I}) P_{int} \quad \text{(A9)}$$

Downloaded from dmd.aspetjournals.org at ASPET Journals on April 10, 2024

DMD Fast Forward. Published on October 23, 2008 as DOI: 10.1124/dmd.108.022483
This article has not been copyedited and formatted. The final version may differ from this version.

$$V_{int}\frac{dMi_{int}}{dt} = f_b\{mi\}CL_{d1}\{mi\}Mi_{intb} + k_a\{mi\}Mi_{lumen}V_{lumen} + f_L CL_{int,met,I}P_{int} - f_L\{mi\}(CL_{d2}\{mi\} + CL_{int,met,I}\{mi\} + CL_{int,sec,I}\{mi\})Mi_{int} \quad (A10)$$

Rates of change of precursor and metabolite in intestine lumen,

$$V_{lumen}\frac{dP_{lumen}}{dt} = -(k_a + k_g)P_{lumen}V_{lumen} + f_L CL_{int,sec,I}P_{int} \quad (A11)$$

$$V_{lumen}\frac{dMi_{lumen}}{dt} = -(k_a\{mi\} + k_g\{mi\})Mi_{lumen}V_{lumen} + f_L\{mi\}CL_{int,sec,I}\{mi\}Mi_{int} \quad (A12)$$

Downloaded from dmd.aspetjournals.org at ASPET Journals on April 10, 2024

Matrix for the TM model: formed metabolite

$$\begin{pmatrix}
\frac{Q_l}{V_R} & -\frac{Q_l}{V_{intb}} & 0 & 0 & 0 & 0 & 0 & 0 \\
-\frac{Q_l}{V_R} & \frac{Q_l + CL_{d1}}{V_{intb}} & -\frac{CL_{d2}}{V_{int}} & 0 & 0 & 0 & 0 & 0 \\
0 & \frac{CL_{d1}}{V_{intb}} & \frac{CL_{int,sec,l} + CL_{int,met,l} + CL_{d2}}{V_{int}} & -k_a & 0 & 0 & 0 & 0 \\
0 & 0 & -\frac{CL_{int,sec,l}}{V_{int}} & k_a + k_g & 0 & 0 & 0 & 0 \\
0 & 0 & 0 & 0 & \frac{Q_l}{V_R} & -\frac{Q_l}{V_{intb}} & 0 & 0 \\
0 & 0 & 0 & 0 & -\frac{Q_l}{V_R} & \frac{Q_i + CL_{d1}\{mi\}}{V_{intb}} & -\frac{CL_{d2}\{mi\}}{V_{int}} & 0 \\
0 & 0 & -\frac{CL_{int,met,l}}{V_{int}} & 0 & 0 & \frac{CL_{d1}\{mi\}}{V_{intb}} & \frac{CL_{int,sec,l}\{mi\} + CL_{int,met,l}\{mi\} + CL_{d2}\{mi\}}{V_{int}} & -k_a\{mi\} \\
0 & 0 & 0 & 0 & 0 & 0 & -\frac{CL_{int,sec,l}\{mi\}}{V_{int}} & k_a\{mi\} + k_g\{mi\}
\end{pmatrix}$$

Downloaded from dmd.aspetjournals.org at ASPET Journals on April 10, 2024

DMD Fast Forward. Published on October 23, 2008 as DOI: 10.1124/dmd.108.022483
This article has not been copyedited and formatted. The final version may differ from this version.

DMD Fast Forward. Published on October 23, 2008 as DOI: 10.1124/dmd.108.022483
This article has not been copyedited and formatted. The final version may differ from this version.

III. SFM: Preformed metabolite

Rate of change of metabolite in reservoir,

$$V_R \frac{dMi_R}{dt} = Q_{sb} Mi_{sb} + Q_{enb} Mi_{enb} - Q_I Mi_R \quad \text{(A13)}$$

Rate of change of metabolite in intestinal serosal blood,

$$V_{sb} \frac{dMi_{sb}}{dt} = Q_{sb}(Mi_R - Mi_{sb}) + f_L\{mi\}CL_{d4}\{mi\}Mi_s - f_b\{mi\}CL_{d3}\{mi\}Mi_{sb} \quad \text{(A14)}$$

Rate of change of metabolite in intestine serosal tissue,

$$V_s \frac{dMi_s}{dt} = f_L\{mi\}CL_{d4}\{mi\}Mi_s - f_b\{mi\}CL_{d3}\{mi\}Mi_{sb} \quad \text{(A15)}$$

Rate of change of metabolite in the blood perfusing the enterocyte layer,

$$V_{enb} \frac{dMi_{enb}}{dt} = Q_{enb}(Mi_R - Mi_{enb}) + f_L\{mi\}CL_{d2}\{mi\}Mi_{en} - f_b\{mi\}CL_{d1}\{mi\}Mi_{enb} \quad \text{(A16)}$$

Rate of change of metabolite in enterocytes,

$$V_{en} \frac{dMi_{en}}{dt} = f_b\{mi\}CL_{d1}\{mi\}Mi_{enb} + k_a\{mi\}Mi_{lumen}V_{lumen} - f_L\{mi\}(CL_{d2}\{mi\} + CL_{int,met,I}\{mi\} + CL_{int,sec,I}\{mi\})Mi_{en} \quad \text{(A17)}$$

Rate of change of metabolite in intestine lumen,

$$V_{lumen} \frac{dMi_{lumen}}{dt} = -(k_a\{mi\} + k_g\{mi\})Mi_{lumen}V_{lumen} + f_L\{mi\}CL_{int,sec,I}\{mi\}Mi_{en} \quad \text{(A18)}$$

Downloaded from dmd.aspetjournals.org at ASPET Journals on April 10, 2024

Matrix for the SFM model: preformed metabolite

$$\begin{pmatrix} \frac{Q_s + Q_{en}}{V_R} & -\frac{Q_s}{V_{sb}} & 0 & -\frac{Q_{en}}{V_{enb}} & 0 & 0 \\ -\frac{Q_s}{V_R} & \frac{Q_s + CL_{d3}\{mi\}}{V_{sb}} & -\frac{CL_{d4}\{mi\}}{V_s} & 0 & 0 & 0 \\ 0 & \frac{CL_{d3}\{mi\}}{V_{sb}} & \frac{CL_{d4}\{mi\}}{V_s} & 0 & 0 & 0 \\ -\frac{Q_{en}}{V_R} & 0 & 0 & \frac{Q_{en} + CL_{d1}\{mi\}}{V_{enb}} & -\frac{CL_{d2}\{mi\}}{V_{en}} & 0 \\ 0 & 0 & 0 & -\frac{CL_{d1}\{mi\}}{V_{enb}} & \frac{CL_{d2}\{mi\} + CL_{int,sec,I}\{mi\} + CL_{int,met,I}\{mi\}}{V_{en}} & -k_a\{mi\} \\ 0 & 0 & 0 & 0 & -\frac{CL_{int,sec,I}\{mi\}}{V_{en}} & k_a\{mi\} + k_g\{mi\} \end{pmatrix}$$

Downloaded from dmd.aspetjournals.org at ASPET Journals on April 10, 2024

DMD Fast Forward. Published on October 23, 2008 as DOI: 10.1124/dmd.108.022483
This article has not been copyedited and formatted. The final version may differ from this version.

DMD Fast Forward. Published on October 23, 2008 as DOI: 10.1124/dmd.108.022483
This article has not been copyedited and formatted. The final version may differ from this version.

IV. SFM: Formed metabolite

Rates of change of precursor and metabolite in reservoir,

$$V_R \frac{dP_R}{dt} = Q_{sb}P_{sb} + Q_{enb}P_{enb} - Q_I P_R \quad \text{(A19)}$$

$$V_R \frac{dMi_R}{dt} = Q_{sb}Mi_{sb} + Q_{enb}Mi_{enb} - Q_I Mi_R \quad \text{(A20)}$$

Rates of change of precursor and metabolite in intestinal serosal blood,

$$V_{sb} \frac{dP_{sb}}{dt} = Q_{sb}(P_R - P_{sb}) + f_L CL_{d4}P_s - f_b CL_{d3}P_{sb} \quad \text{(A21)}$$

$$V_{sb} \frac{dMi_{sb}}{dt} = Q_{sb}(Mi_R - Mi_{sb}) + f_L\{mi\}CL_{d4}\{mi\}Mi_s - f_b\{mi\}CL_{d3}\{mi\}Mi_{sb} \quad \text{(A22)}$$

Rates of change of precursor and metabolite in intestine serosal tissue,

$$V_s \frac{dP_s}{dt} = f_L CL_{d4}P_s - f_b CL_{d3}P_{sb} \quad \text{(A23)}$$

$$V_s \frac{dMi_s}{dt} = f_L\{mi\}CL_{d4}\{mi\}Mi_s - f_b\{mi\}CL_{d3}\{mi\}Mi_{sb} \quad \text{(A24)}$$

Rates of change of of precursor and metabolite in the blood perfusing the enterocyte layer,

$$V_{enb} \frac{dP_{enb}}{dt} = Q_{enb}(P_R - P_{enb}) + f_L CL_{d2}P_{en} - f_b CL_{d1}P_{enb} \quad \text{(A25)}$$

$$V_{enb} \frac{dMi_{enb}}{dt} = Q_{enb}(Mi_R - Mi_{enb}) + f_L\{mi\}CL_{d2}\{mi\}Mi_{en} - f_b\{mi\}CL_{d1}\{mi\}Mi_{enb} \quad \text{(A26)}$$

Rates of change of precursor and metabolite in enterocytes,

$$V_{en} \frac{dP_{en}}{dt} = f_b CL_{d1}P_{enb} + k_a P_{lumen}V_{lumen} - f_L(CL_{d2} + CL_{int,met,I} + CL_{int,sec,I})P_{en} \quad \text{(A27)}$$

$$V_{en} \frac{dMi_{en}}{dt} = f_b\{mi\}CL_{d1}\{mi\}Mi_{enb} + k_a\{mi\}Mi_{lumen}V_{lumen} + f_L CL_{int,met,I}P_{en} - f_L\{mi\}(CL_{d2}\{mi\} + CL_{int,met,I}\{mi\} + CL_{int,sec,I}\{mi\})Mi_{en} \quad \text{(A28)}$$

Rate of change of precursor and metabolite in intestine lumen,

Downloaded from dmd.aspetjournals.org at ASPET Journals on April 10, 2024

DMD Fast Forward. Published on October 23, 2008 as DOI: 10.1124/dmd.108.022483
This article has not been copyedited and formatted. The final version may differ from this version.

$$V_{lumen}\frac{dP_{lumen}}{dt} = -(k_a + k_g)P_{lumen}V_{lumen} + f_L CL_{int,sec,I}P_{en} \quad \text{(A29)}$$

$$V_{lumen}\frac{dMi_{lumen}}{dt} = -(k_a\{mi\} + k_g\{mi\})Mi_{lumen}V_{lumen} + f_L\{mi\}CL_{int,sec,I}\{mi\}Mi_{en} \quad \text{(A30)}$$

Downloaded from dmd.aspetjournals.org at ASPET Journals on April 10, 2024

Matrix for the SFM model: formed metabolite

$$\begin{pmatrix}
\frac{Q_s + Q_{en}}{V_R} & -\frac{Q_s}{V_{sb}} & 0 & -\frac{Q_{en}}{V_{enb}} & 0 & 0 & 0 & 0 & 0 & 0 & 0 & 0 \\
-\frac{Q_s}{V_R} & \frac{Q_s + CL_{d3}}{V_{sb}} & -\frac{CL_{d4}}{V_s} & 0 & 0 & 0 & 0 & 0 & 0 & 0 & 0 & 0 \\
0 & \frac{CL_{d3}}{V_{sb}} & \frac{CL_{d4}}{V_s} & 0 & 0 & 0 & 0 & 0 & 0 & 0 & 0 & 0 \\
-\frac{Q_{en}}{V_R} & 0 & 0 & \frac{Q_{en} + CL_{d1}}{V_{enb}} & -\frac{CL_{d2}}{V_{en}} & 0 & 0 & 0 & 0 & 0 & 0 & 0 \\
0 & 0 & 0 & -\frac{CL_{d1}}{V_{enb}} & \frac{CL_{d2} + CL_{int,sec,I} + CL_{int,met,I}}{V_{en}} & -k_a & 0 & 0 & 0 & 0 & 0 & 0 \\
0 & 0 & 0 & 0 & -\frac{CL_{int,sec,I}}{V_{en}} & k_a + k_g & 0 & 0 & 0 & 0 & 0 & 0 \\
0 & 0 & 0 & 0 & 0 & 0 & \frac{Q_s + Q_{en}}{V_R} & -\frac{Q_s}{V_{sb}} & 0 & -\frac{Q_{en}}{V_{enb}} & 0 & 0 \\
0 & 0 & 0 & 0 & 0 & 0 & -\frac{Q_s}{V_R} & \frac{CL_{d3}\{mi\} + Q_s}{V_{sb}} & -\frac{CL_{d4}\{mi\}}{V_s} & 0 & 0 & 0 \\
0 & 0 & 0 & 0 & 0 & 0 & 0 & -\frac{CL_{d3}\{mi\}}{V_{sb}} & \frac{CL_{d4}\{mi\}}{V_s} & 0 & 0 & 0 \\
0 & 0 & 0 & 0 & 0 & 0 & -\frac{Q_{en}}{V_R} & 0 & 0 & \frac{CL_{d1}\{mi\} + Q_{en}}{V_{enb}} & -\frac{CL_{d2}\{mi\}}{V_{en}} & 0 \\
0 & 0 & 0 & 0 & -\frac{CL_{int,met,I}}{V_{en}} & 0 & 0 & 0 & 0 & -\frac{CL_{d1}\{mi\}}{V_{enb}} & \frac{CL_{d2}\{mi\} + CL_{int,sec,I}\{mi\} + CL_{int,met,I}\{mi\}}{V_{en}} & -k_a\{mi\} \\
0 & 0 & 0 & 0 & 0 & 0 & 0 & 0 & 0 & 0 & -\frac{CL_{int,sec,I}\{mi\}}{V_{en}} & k_a\{mi\} + k_g\{mi\}
\end{pmatrix}$$

Downloaded from dmd.aspetjournals.org at ASPET Journals on April 10, 2024

DMD Fast Forward. Published on October 23, 2008 as DOI: 10.1124/dmd.108.022483
This article has not been copyedited and formatted. The final version may differ from this version.